Stratigraphic heterogeneity of a Holocene ooid tidal sand shoal:
Lily Bank, Bahamas

by

Andrew G. Sparks
B.A., Franklin & Marshall College, 2008

Submitted to the Department of Geology
and the Faculty of the Graduate School of The University of Kansas
in partial fulfillment of the requirements for the degree of
Master of Science
2011

Advisory Committee:

_____
Eugene C. Rankey, Chair

_____
Georgios P. Tsoflias

_____
Krishnan Srinivasan

Date Defended: _____

The Thesis Committee for Andrew G. Sparks certifies that this is the approved version of the following thesis:

Stratigraphic heterogeneity of a Holocene ooid tidal sand shoal:
Lily Bank, Bahamas

Advisory Committee:

_____
Eugene C. Rankey, Chair

Date Approved: _____

ABSTRACT

A central challenge in sedimentary geology is understanding three-dimensional architectural variability, and how it might be predicted. Ooid sand shoals, present in the stratigraphic record from Archean to recent, represent an economically important, but heterogeneous type of carbonate deposit. Whereas the processes influencing the deposition of ooid shoals are well examined and understood, the means by which distinct processes are recorded in the rock record are less constrained. The purpose of this thesis is to understand the relationship among processes, plan-view morphology and stratigraphic variability by examining Lily Bank, a modern tidally dominated Bahamian ooid shoal. Research focuses on two bar form end-members of Lily Bank: transverse shoulder bars oriented normal to flow and flood- and ebb-tide oriented parabolic bars. Results from integrating remote sensing imagery, high frequency seismic (Chirp) data and core characterization (sedimentary structures and granulometric analyses) reveal the stratigraphic record of geomorphic change. An irregular, but gently dipping surface acts as the base of the Holocene sequence. This lowest horizon (Z) is interpreted as the Top Pleistocene and shallows onto the platform. A lower unit (Unit A), up to 6 m thick, overlies this basal surface and is characterized as a poorly sorted gravelly muddy sand with abundant *Halimeda*, and almost no ooids. Unit A is capped by a transitional unit (Unit B) which shows an increase in ooids, better sorting, and larger grain sizes upwards. The uppermost unit (Unit B'), present only under the present-day bar forms, is a well-sorted ooid sand. Quantitative analysis reveals quantitative relations among units, geomorphic position, and granulometry. Sediments of Unit A are finer and less well sorted than those from Unit B. Likewise, the fraction of grains larger than 500 μm and sorting of sediments from crests of bar forms are clearly differentiated from those on the bar flanks. Collectively, these results provide more robust three-dimensional conceptual models of heterogeneity in ooid shoals.

ACKNOWLEDGEMENTS

I am grateful to numerous people who have aided in the completion of this project. Dr. Eugene C. Rankey has been invaluable both as my advisor and as a mentor. I would also like to thank Krishnan Srinivasan and George Tsoflias, who serve on my committee, for their patience, guidance, and insight. Barry Albury provided immense help in field work and for use of his vessel. I'd like to thank Humberto Guarin and Jason Rush for helping with data acquisition, processing and interpretation; their involvement kept the project moving during difficult times. The project was graciously funded by the National Science Foundation (Grant # EAR-0922122) and the Geological Society of America (GSA). Ian Rowell, Dr. Paul Enos, and Dr. Bill Johnson were also helpful with their lab input, logistical advice and other various insights. Roland Albury of the Department of Fisheries of The Bahamas is acknowledged for allowing research in the area. Finally, I'd like to thank my wife, Laura, for her support and encouragement throughout the project's duration.

Table of Contents

INTRODUCTION

Stratigraphy represents the preserved net accumulated product of a diverse suite of depositional and erosional sedimentary processes. In carbonate successions, these processes include creation, transport, and dimunition of sediment, construction of *in situ* biologic structures, and erosion of previously deposited sediment. These diverse processes commonly lead to a complex stratigraphic record marked by considerable heterogeneity at several scales.

Oolitic sands are one type of heterogeneous carbonate accumulation, and can be found in strata of almost any age, from Archean to recent (e.g., Wilson, 1975; Opdyke and Wilkinson, 1990; Sumner and Grotzinger, 1993). One means to explore heterogeneity that could be present in ancient analogs is to examine and map spatial patterns of Holocene systems (Ginsburg, 1956; Enos, 1977; Purkis et al., 2005; Rankey et al., 2006; Harris and Vlaswinkel, 2008; Harris and Ellis, 2009; Harris 2010). More recently, the role of hydrodynamic influences on oolitic systems has been explored systematically (Gonzalez and Eberli, 1997; Rankey and Reeder, 2008; Rankey and Reeder, 2011). Collectively, these studies have elucidated the spatial patterns of accumulation, the processes that shape oolitic systems, and the role of feedbacks. What remain unclear, however, are the details of shoal evolution - how do shoals with different geometries arise, change and evolve? And, for the geologist, how might these processes and depositional geometries be recognized from the stratigraphic record of ancient shoals? Whereas the patterns and the causative processes in shoal systems are not random, there have been few systematic efforts to directly and explicitly link the details of processes, Holocene shoal geometries, and their potential stratigraphic record. Yet, this information is central for accurate and meaningful interpretation of the Earth surface processes that generated, and can be reflected in, ancient analogs and their potential stratigraphic heterogeneity.

In this context, this project aims to take the logical next step in studying ooid sand shoals, exploring how shoals with different formative processes and geomorphology create their stratigraphic record. Specifically, by examining Lily Bank, a Holocene marine sand belt in which the linked roles of tides, waves, and sediment transport on geomorphology are well constrained, this project tests several

linked hypotheses: 1) the subsurface sedimentology and stratigraphy of distinct geomorphic positions reflect variable depositional processes; and, if present, 2) the different subsurface patterns are distinct from other geomorphic positions. The importance of these insights lies in providing new perspective into the relations between facies bodies and depositional porosity and permeability, which could be used to refine facies models or conceptual models of subsurface heterogeneity.

STUDY AREA AND SETTING

Lily Bank is situated along the northeastern edge of Little Bahama Bank (LBB), an isolated carbonate platform in the northern Bahamas. Along the northern margin of LBB facing the open Atlantic Ocean, the Abaco island chain extends over 100 km (Hine, 1977; Rankey et al., 2006; Reeder and Rankey, 2009), and consists of Pleistocene bedrock outcrops. Just north of this island chain are discontinuous Holocene reefs, flanked by a narrow back-reef shelf. These barriers, including the reefs and islands, restrict and focus tidal energy, facilitating the growth of sand shoals (Hine, 1977; Reeder and Rankey, 2008). LBB also contains a muddy lagoon on the protected, platformward side of the islands, deltas, sand shoals, and patch reefs (Fig. 1).

One of these sand shoals, Lily Bank, is a tidally dominated marine sand belt (Ball, 1967) extending 27 km along strike and ~4 km across, generally parallelling the northern margin of LBB. The active ooid shoal occurs on the shallow platform top, ~12 km back from the shelf margin. Hine (1977) subdivided Lily Bank into three general geomorphic regions: 1) downdip flow-parallel inactive tidal sand ridges, which have crests (shallowest parts of bar forms) in 3-5 m water depth, 2) platformward inactive subaqueous dunes, and 3) the updip active shoal (Lily Bank itself and the focus of this study) (Fig. 1). The tidal amplitude in this area ranges from 61 cm during neap tides to 108 cm in spring tides (Rankey and Reeder, 2011).

The active part of Lily Bank includes variable bar forms, which are clearly distinguishable on the remote sensing data (Fig. 2), related to the patterns of tidal flow (Hine, 1977; Rankey et al., 2006; Rankey

and Reeder, 2011). One bar form end member, parabolic bars, can vary from isolated asymmetric bar forms, to linked parabolic bars that collectively form a sinusoidal trend, to nearly symmetrical parabolic bars (Fig. 2). Superimposed on the parabolic bars are subaqueous dunes with variable orientations, from normal to the central axis at the crest apex, to oblique to the central crest on the crest flanks. The parabolic bars reach ~3 m of maximum bathymetric relief with apertures between crest flanks ranging from 0.7 to 3.3 km and amplitudes between crest apexes of up to 2 km (Rankey and Reeder, 2011).

One region illustrates the general tidal flow patterns associated with parabolic bars (Fig. 2). In this area, a southward (flood) oriented (Fig. 2) parabolic bar is flanked by a juxtaposed northward (ebb) oriented parabolic bar. During flood tide, flow is funneled through the flood oriented bar, narrowing to its apex and dispersing (Rankey and Reeder, 2011). In contrast, during ebb tide, flow is diverted around the flood bar apexes, and is focused through the ebb-oriented bar (Rankey and Reeder, 2011). This mutually evasive, tidally dominated circulation causes migration of both flood- and ebb-oriented subaqueous dunes and bar forms in opposite directions, even though the shoal-scale net transport is in the platformward (flood) direction (Hine, 1977; Rankey and Reeder, 2011).

In contrast to parabolic bars, transverse shoulder bars (the 'ramps' of Hine, 1977; Fig. 2), the other Lily Bank bar form end member, are oriented perpendicular to highly oblique to flow. Most subaqueous dunes superimposed on transverse shoulder bars are oriented parallel to the long axis of the bar, and are flood oriented. These bar forms can have up to 3 m of relief, have spacing of ~1 km from crest flank to crest, and extend nearly 2 km along strike (Rankey and Reeder, 2011).

In the focus area, in addition to flood-dominated subaqueous dunes, transverse shoulder bars include well-defined stoss (north) and lee (south) flanks, suggesting the dominance of flood tides. During flood tide, flow moves up the bar form, increasing in speed with progressive vertical restriction, reaching 70-80 cm sec^{-1} (Rankey et al., 2006). Once over the crest, flow dissipates due to deeper water and limited vertical restriction, and speeds drop abruptly. During ebb tide, dominant currents are deflected by transverse shoulder bar crests, and flow parallel to the bar axis (Rankey et al., 2006).

In sum, the distinct bar forms include different relations between bar form geomorphology and tidal flow patterns. The stratigraphic record of these processes and bar forms is the focus of this study.

METHODS

Over 16 line-km of Chirp sub-bottom profiles (Fig. 3) were acquired on a series of strike- and dip-oriented lines with ~200 m spacing using Edge-Tech X-Star full-spectrum digital subbottom profiler (500 Hz – 12 kHz) mounted on a small catamaran. This wideband FM high-resolution subbottom profiler generates cross-sectional images below the seabed using a chirp technique (stepped FM) to minimize multipath and noise effects. This system uses matched filter correlation and waveform-weighted techniques that result in high-resolution profiling with virtually constant resolution with depth. To maintain accurate positioning, the data acquisition system was integrated with a Trimble series 4000 DGPS (Rankey et al., 2009). Interpretation utilized standard geophysical interpretation software. All depths and thicknesses were estimated from the seismic data using the speed of sound in unconsolidated carbonates (1650 m/s; Incze, 1998) and the speed of sound through water (1500 m/s; Shinn et al., 1990).

Preliminary interpretations of Chirp subbottom profiles (see **Seismic** section below) guided coring locations, with the general goal of capturing geomorphological and sedimentological variability within and between bar forms. A SCUBA team used a vibracore and a custom 6-m tripod system to collect 27 m of sediment from nine cores on Lily Bank (Fig. 3), ranging in length from 0.95 m to 4.45 m of (1.34 – 6.27 m decompacted, 17.68% average compaction) sediment (Appendix A includes descriptions of all cores). Thicknesses and depths reported here are decompacted values.

Following transport back to the lab, cores were cut into meter-long sections with a chop-saw, whereupon they were frozen, and cut longitudinally using a table saw. Each core was described and photographed for archiving purposes. Grain sizes of samples every 5 cm from each core were analyzed systematically using a sonic sieve; granulometry was captured using a standard statistics package (Gradistat; Blott, 2000). Results are reported using standard measures for sorting (Folk and Ward, 1957)

and textural classification (Folk, 1954). Key cores (n = 8) were sampled for petrographic study (n = 149 total thin sections), and semi-quantitatively analyzed using standard comparators to estimate the abundance of different grain types within and among cores (Appendix B includes all quantitative data from cores and thin sections).

Following analysis of the cores, the core data were re-integrated with the sub-bottom profiles and interpretations were refined. Integration focused on evaluating the geological meaning of the reflections by linking seismic character to the sedimentology and stratigraphy of the Holocene succession.

SEISMIC CHARACTERISTICS OF OOID SHOALS

Internal Seismic Character

Seismic data shed light on subsurface variability of reflectors, internal geometries, and sediment packages. Illustrative seismic lines from a transverse shoulder bar (Fig. 4) and a parabolic bar (Fig. 5) show the general seismic character of the Holocene succession across the study area.

A line across the transverse shoulder bar (Fig. 4) includes five reflectors that break the succession into three seismic packages, although the uppermost unit locally can be further separated into two seismic units. The basal reflector (Reflector Z) is a weak to moderate amplitude, continuous, flat horizon. Reflector Z can be traced across the line, but generally has higher amplitude lagoonward. This reflector occurs at ~9 - 11 m, a depth coincident with the hard, rocky substrate exposed regionally downdip (Fig. 1). Overlying Reflector Z is a second, moderate to high amplitude, continuous horizon (Reflector A). Reflector A is traceable across the line, and locally converges and diverges with underlying Reflector Z. Overlying Reflector A is Reflector B. Reflector B is a low- to moderate-amplitude, apparently continuous reflector, but is masked by the seafloor multiple under the bar forms in some areas. This reflector is strongest and more easily traced in the inter-bar channel and becomes ambiguous in the lagoon. The fourth reflector (Reflector B') is characterized by a moderate- to high-amplitude horizon that occurs only under the active bar forms. In the inter-bar channel and in lagoonal areas, Reflector B'

merges with the sediment-water interface and therefore is absent in these areas. The shallowest reflector (Reflector C) is the present day sediment-water interface.

These reflectors define several seismic stratigraphic units. The basal unit (Unit Z) overlies Reflector Z and is capped by Reflector A. Unit Z has variable thicknesses and is characterized by a strong seismic response. The middle unit (Unit A) is bound below by Reflector A and above by Reflector B. Unit A is a generally sheet-like deposit that contains a weak, seismically transparent signature distinct from Unit Z. On this line, locally the uppermost unit (Unit B) is separated into Unit B and Unit B'. Unit B overlies Reflector B and is capped by either Reflector B' (under the active bar forms) or the sediment-water interface in the inter-bar channel and lagoon. This unit is thinner than Unit A but contains a stronger seismic response with more marked reflectors. Capping the succession, Unit B' is the found only under the active bar forms. Rarely in this line, Unit B' includes high-amplitude reflectors that decrease in dip downward and are tangential to Reflector B.

A representative line across a flood-oriented parabolic bar (Fig. 5) shows seismic features similar to those evident in the transverse shoulder bar. Reflectors Z, A, B, B' and C were carried across the survey area and loop tied, and break the seismic succession of the parabolic bar into three distinct units: 1) the basal, seismically strong unit with variable thickness (Unit Z), 2) the sheet-like, seismically transparent Unit A, and 3) a Unit B with variable thickness. On this line, Unit B is split by Reflector B', expressed here as a moderate- to high-amplitude reflector under bar forms. Unit B' includes shingled internal geometries across the area. Although these reflectors are best expressed within Unit B', some of the reflectors appear to continue into Unit B (Fig. 5 C). The shingled geometry within Unit B' are better defined and more prevalent in the parabolic bars than in the transverse shoulder bars. Within the parabolic bars, the dip direction of the downlapping reflectors (here, to the south, or platformward) are consistent with the direction of bar form migration (flood-oriented) interpreted from their geomorphic expression (Rankey et al., 2006).

Regional Trends in Reflectors and Units

Synthesizing data from all the seismic lines reveals trends in depth for each reflector and thickness and distribution for each seismic unit. Across much of the area, the basal reflector (Reflector Z) occurs at depths ranging from 9.1 m to 11.4 m (Fig 6A). Regionally, Reflector Z is shallowest under the crest of the southwestern-most transverse shoulder bar, and reaches its greatest depths under the parabolic bars to the east. Although there is a first-order trend that reveals that Reflector Z shallows from north to south or northeast to southwest across the study area, there is no marked topographic high or bump underneath the shoal itself (cf. Purdy, 1961). The overlying reflector, Reflector A, ranges in depths from 8.0 m to 9.3 m. Regionally and locally, this horizon mimics the trends observed in Reflector Z; Reflector A is shallowest in the west, under the southwestern transverse shoulder bar, and generally is deeper under the parabolic bars to the east. The next reflector, Reflector B, ranges in depths from 3.9 m to 8.0 m (Fig. 6B). The reflector reaches its shallowest depth under the southwestern transverse shoulder bar, but generally deepens to the north and east, reaching its deepest in the northeast and in the lagoon. Within individual bar forms (especially evident in association with the transverse shoulder bars), Reflector B is shallowest under the crest, and gradually deepens down the barforms. Reflector B' ranges in depths from 3.5 m to 6.0 m (Fig. 6C). Regionally it is shallowest under the southwestern-most transverse shoulder bar and deepens to the northeast. Under individual bar forms, Reflector B' (like Reflector B) shallows under the crest and deepens down the bar forms (compare with Figure 4B). Reflector C, the sediment-water interface, reaches depths of 1.0 m on the crest of the bar forms, whereas in the lagoon, it lies ~5.5 m below sea level.

These changes in reflector depths are associated with changes in thicknesses of each of the seismic units. For example, Unit A, which is bound by Reflectors A and B, ranges in thickness from 1.8 m to 5.8 m (thickest under the parabolic bars) (Fig. 6D). This unit is generally thinnest in the lagoon and inter-bar channel while thickening under the active bar forms.

The upper unit, Unit B (including capping Unit B', where present) is bound below by Reflector B and above by the present-day sea floor. This unit ranges in thickness from 0.3 m to 4.2 m (Fig. 6E). Unit

B is the thickest in the inter-bar channel and under the parabolic bars, and thins under the bar crests. Unit B', which overlies Reflector B' (where present), is capped by the sediment-water interface and is absent in the inter-bar channel and in the lagoon. This unit, present only under the active bar forms, reaches thicknesses of up to 3.8 m (Fig. 6F). Where present, this unit is generally thickest under the transverse shoulder bars and thins to the east under the parabolic bar forms and closer to the inter-bar channel and lagoon. Locally, within each bar form, this subunit thickens under the crest of the bar forms and thins distally.

SEDIMENTOLOGY OF THE HOLOCENE SUCCESSION

Cores provide details on the sedimentologic and stratigraphic variability within and among the distinct bar forms and provide ground truth for seismic data. Core data described in the context of their location illustrate changes in sedimentology and stratigraphy with geomorphic context.

Lagoon Sedimentology and Stratigraphy

The core from the lagoon penetrated to a depth of 1.95 m, and includes sediments that vary only subtly with depth (Figs. 3, 7; LBR 3.4). The lagoonal core sediment is dominated by poorly to very poorly sorted (3.58 - 5.07 Φ), burrowed, gravelly to slightly gravelly muddy sand (classification here and hereafter follows Folk and Ward, 1957; Folk, 1954). The abundance of *Halimeda* flakes (~ 12-15%) and skeletal fragments including bivalves (10%), forams (5-8%) and gastropods (1-2%) remains similar throughout this core. The sediments are bioturbated throughout, although the middle of the core contains less intense burrowing. The top 20 cm of the core also includes sea grass. The lagoonal core includes almost no ooids, which comprise roughly 1% of the sediment throughout the core (Fig. 7). Granulometrically, the base of the core is dominated by coarse sand, with a mean grain size of 512 μm (classification of Wentworth, 1922, here and hereafter), but gradually fines upwards (increasing in mud

content) to fine sand with an mean grain size of 245 µm at the top, showing an overall fining upward succession.

Channel (Inter-bar) Sedimentology and Stratigraphy

A representative core from a channel between transverse shoulder bars reached 4.1 m in depth and includes two distinct units (Figs. 3, 8; LBR 1.4). The bottom unit of the core includes a basal 10 cm gravelly sand dominated by shell fragments of bivalves, gastropods, and forams, with scattered intraclasts and *Halimeda*. Mean grain size is 350 µm (medium sand), mud ranges between 5 – 10%. Ooids, absent at the base, increase in abundance to comprise ~10% of the sediment at the top of the unit. This lower unit passes sharply up into a ~1.5 m thick, poorly to very poorly sorted (2.27 Φ - 4.25 Φ), burrowed, gravelly muddy sand dominated by peloids, with interbedded thin (~ 2 cm) *Halimeda*-rich layers. Within this unit, mean grain size ranges from 419 µm (medium sand) at the base to 321 µm (medium sand) at the top.

A rapid shift occurs in the sedimentology of the core at ~2.4 m depth, and sediments above are distinct from those below. Here, ooid abundance increases gradually upwards, from ~10% at at the contact to ~ 50% at the top of the core. Granulometrically, the sand content increases from 89% below the contact to 95% just above, whereas gravel content decreases from 16% below the contact to 2% above and mud continues to decrease. The mean grain size increases from 277 µm at the base of the upper unit to 315 µm at the top of the core. The top 1 m of the core is an ooid - peloid - skeletal gravelly sand with *in situ* sea grass roots and shows a mixing of sand, gravel, and mud content.

Transverse Shoulder Bar Sedimentology and Stratigraphy

A representative core from the flank of a transverse shoulder bar (Figs. 3, 9; LBR 1.3) penetrated 6.2 m, almost reaching Reflector A from the seismic data. At the base of the core, a 10 cm unit of gravel-sized bivalve and grastropod fragments (top of Unit A??) is sharply overlain by a ~2.0 m thick poorly

sorted (2.15 Φ - 3.06 Φ) bioturbated slightly gravelly muddy sand dominated by peloids and *Halimeda* (Figs. 10A,B). This lower unit includes very few (< 5%) ooids. This lower unit has a mean grain size of approximately 365 µm (medium sand), and is broadly similar to sediments in the cores from channel and lagoonal areas. Similarly, like the sediments from the lagoon and channel, the granulometry is variable – sand ranges in abundance from 83-93%, whereas the mud ranges from 4-9%, (average 6%), and gravel ranges from 0-13% (average 6%).

The lower slightly gravelly muddy sand abruptly passes into a second, thinner, transitional unit at ~4.1 m core depth, becoming predominantly clean sand. This lower contact is marked by a change in ooid abundance as ooids increase from 5% of the sediments below to ~30% just above the contact. Ooids continue to increase in abundance to ~ 50% at the top of this unit. Similar to the increase in ooid abundance, the mean grain size increases from 360 µm below the contact to 530 µm just above, but fines to 403 µm at the top of this unit. Sorting improves throughout this section from 2.42 Φ (poorly sorted) to 1.9 Φ (moderately sorted) at the top of the unit. The granulometry also changes; sand content increases from 84% at the base of this transitional unit to 96% at the top, as mud and gravel content decreases to < 4% upwards. Sedimentologically, this unit is similar to the top unit seen in the inter-bar channel core (Fig. 8).

Unlike the successions in the lagoon or inter-bar channel, the transverse shoulder bar also includes an upper, sedimentologically distinct unit. Above the contact, this upper unit of medium sand (mean size 418 µm) is dominated by ooids (Fig. 10C). Whereas the lower unit contains < 5% ooids, increasing abruptly in the transitional unit to 30% ooids, ooid abundance in the upper units starts at 50% and continues to gradually increase upwards to ~80% at the top of the core. Across the contact between transitional and upper units, the granulometry of the core changes abruptly. Here, the abundance of sand increases upwards, from 93% to nearly 100%, whereas the amount of mud and gravel decreases from ~5% to close to 0%, keeping constant to the top of the core. The sorting of the upper unit also varies; the

base is moderately sorted (1.98 Φ) whereas the top of the unit is well sorted (1.4 Φ). The upper 1.2 m of the core includes the most ubiquitous ooids, the best sorting, and the most homogenous granulometry.

A core from the crest of the transverse shoulder bar penetrated through the upper unit and transitional unit, (Fig. 11; LBR 1.3), although it failed to penetrate the lower gravelly muddy sand unit evident in the other cores. This core includes the transitional unit that increases in ooid abundance upwards, from 2% ooids to 10% ooids, with between 0-9% gravel, 2-6% mud, and 87-96% sand. Mean grain size decreases from 332 μm (medium sand) at the base of this transitional unit to 217 μm at the top (fine sand). Sorting is relatively constant through the interval, fluctuating from 2.42 Φ to 2.26 Φ (poorly sorted). A contact is marked at the top of this transitional unit by a rapid change in granulometric properties. The amount of gravel decreases from 9% below the contact to 2% above, whereas sand increases from 86% to 91% over that same interval. Ooids continue to increase upwards in the upper unit, from 12% at the base, to 80%, dominating the sediment at the top of the core. This upper unit also increases in mean grain size upwards, as the grain sizes range from 281 μm (fine sand) at the base of the unit, to 524 μm (coarse sand) at the top. Sorting also improves in this unit, from 2.27 Φ (poorly sorted) at the base, to 1.69 (moderately sorted) at the top. Similar to the transverse shoulder bar flank core, the upper unit can be further subdivided into smaller units (grey dashed lines) based on ooid abundance and granulometric properties.

Parabolic Bar Sedimentology and Stratigraphy

A representative core from a parabolic bar (Fig. 12; LBP 1.2) contains lower, transitional, and upper units broadly comparable to the transverse shoulder bar. This core penetrated 4.63 m of sediment, but did not encounter bedrock. The lower unit of the parabolic bar is a ~1.5 m thick, poorly sorted (2.16 Φ - 3.45 Φ) bioturbated gravelly muddy sand dominated by peloids, *Halimeda*, forams, and bivalve fragments (Fig. 10D, E) with scattered muddy intraclasts. Similar to the lower unit in transverse shoulder bars, this unit in the parabolic bar is a medium sand (mean size ~ 300 μm) containing few (< 5%) ooids.

As in the transverse shoulder bar, the lower unit has variable granulometry, and ranges from 86-96% sand, 4-9% mud, and 0-9% gravel.

Comparable to the transverse shoulder bar, a transitional zone 1.2 m thick overlies the lowest unit. Ooid abundance increases from 2% above the lower contact to 20% at the top of the transitional unit. Overall, mean grain size in the transitional unit is similar to that in the lower unit, averaging ~300 μm (medium sand). Sorting improves in this unit, from 3.5 Φ at its base to 2.7 Φ upwards (both poorly sorted). In this zone, the sand increases from ~83% to ~92%. Oppositely, the gravel content decreases from 10% to ~2% whereas the mud content is between 5 – 10%.

The uppermost unit capping the parabolic bar core is marked by a significant increase in ooids and change in granulometry. The top of the transitional unit contains 25% ooids, whereas the base of the upper unit has more than 50% ooids. The upper unit continues to increase in ooid abundance to ~75% at the top of the core. Mean grain size remains similar to the rest of the core, averaging ~300 μm, but increases to a mean of 415 μm (medium sand) at the very top of the core, corresponding to the increase in ooid abundance (Fig. 10F). Sorting improves throughout this unit, from 2.4 Φ (poorly sorted) at its base to 1.8 Φ (moderately sorted) towards the top of the core. The base of this moderately sorted upper unit contains horizontal laminations dominated by ooids with some *Halimeda* and peloids. These sediments pass upwards to trough cross-laminations dominated by ooids with some peloids, *Halimeda*, and skeletal fragments. Granulometry also sees a marked shift; sand abundance increases from ~94% at the base of the upper unit to ~98% at the top, as mud decreases from ~5% to close to 0% at the top. Gravel increases from ~ 0% to ~5% at the top.

Repeated attempts at collecting a deep core from the crest of the parabolic bar were unsuccessful due to the presence of a continuous hardground, but a shallow (1.34 m) core from there provides sedimentologic information on the character of the sediments there (Fig. 13; LBP 1.1). This sand is dominated by ooids, consistently over 60% in abundance, but also contains ~20% peloids, ~8 % *Halimeda* fragments and other skeletal fragments. There is no gravel, and very little (< 4%) mud

throughout this core. The mean grain size of the core as a whole is 688 μm (coarse to very coarse sand) and sediments are moderately sorted (average sorting of 1.83 Φ).

INTEGRATION OF SEISMIC GEOMETRIES WITH HOLOCENE SEDIMENTOLOGY

Integration of Chirp sub-bottom data with sedimentologic and stratigraphic patterns in the cores provides a unique perspective on variability and heterogeneity in this Holocene succession (Fig. 14). As discussed above, the basal seismic horizon, Reflector Z, occurs at depths comparable to that of a hard, rocky substrate exposed regionally, including areas outboard of Lily Bank (Fig. 1; Fig. 14). Based on its depth, continuity, and occurrence as the deepest reflector, Reflector Z is interpreted to represent the top-Pleistocene surface. Note, however, that cores of Lily Bank did not penetrate to this depth, and bedrock has not been sampled or age-dated. This surface is overlain by Unit Z, which varies in thickness. Based on analogy with other areas (Wanless and Tagett, 1988; Jackson, 1995; Morgan, 2008), this unit may represent a transgressive lag, although no cores penetrate this layer (Fig. 14).

Overlying reflector A is the ~1.5 m thick, seismically transparent Unit A (Fig. 10A-B; Fig. 10D-E; Fig. 14A-B). This unit is generally sheet-like across the area, although it appears to thin over the subtle highs in the top of the Pleistocene (e.g., under the southern bar in Fig. 14A). Sedimentological characterization of this unit from cores reveals that it includes burrowed gravelly muddy sand dominated by peloids with some skeletal fragments, and almost no ooids (Lower Unit in Figs. 8-9, 11-12). Although the sand varies slightly in composition and texture, there are no laterally persistent units with abrupt changes in grain size, sorting or composition that would cause an impedance contrast. The seismically transparent character of Unit A is probably caused by this homogenous sedimentologic character and the intense bioturbation.

Overlying Unit A is Reflector B. Reflector B is continuous throughout the area (Fig. 14). Tying cores to seismic reveal that the depth of this reflector in the seismic data is coincident with the abrupt sedimentological change evident in the cores from the lower unit with no ooids (Unit A) to the upper ooid-rich unit (Unit B; Transitional Unit in Figs. 9,11-12). These sedimentological changes - the increase

in ooids, the change in grain size, and decrease in bioturbation intensity - are interpreted to cause a change in impedance from the sand below to the sand above, and form the interface evident in the seismic data as Reflector B (Fig. 14C, D).

The next horizon, Reflector B', is continuous under the active bar forms but merges with the sediment-water interface in deeper-water areas between the bar forms and in the lagoon (Fig. 14C-D). This unit (Unit B'; Upper Unit in Figs. 8-9, 11-13) is differentiated by a sharp increase in ooid abundance, and changes in grain size and sorting, relative to the underlying transitional unit (Fig. 14A- B). Similarly, the well-defined inclined, lateral accretion surfaces imaged on the seismic data (Fig. 5) are associated with this ooid-dominated sand (Fig. 14A-B), but some appear to continue through the reflector. On the basis of these observations, Reflector B' is interpreted to represent a facies transition between the interval with upwards increase in ooids and sorting (Unit B) and clean ooid sand (Unit B'). This transition is interpreted to represent the lateral change from ooid sand shoal itself to the shoal flank and adjacent channel, as bar forms migrated across the area. Based on similarities in sediment sizes and types off the flank of extant bar forms and the transitional oolitic unit in the cores, the individual foresets evident in Unit B are interpreted to simply pass downdip and laterally into more homogenous sediments with less impedance contrast (hence, lose seismic definition) rather than downlap onto Reflector B.

STRATIGRAPHY, GEOMORPHOLOGY, AND SEDIMENTOLOGICAL VARIABILITY

Core data demonstrate distinctions among sediment types, sizes, and sorting as stratigraphy and geomorphology change. A comparison between sedimentologic attributes of Unit A, Unit B, and Unit B' reveals distinct ranges of grain sizes and sorting for each (Fig. 15A). The sediments in the lower unit, Unit A, show high variability, with mean size ranging from 212 - 1089 μm, with a median of 333 μm (medium sand). Unit A also has variable sorting, ranging from 1.5 Φ to 5.0 Φ (moderately to very poorly sorted). The other sedimentologic end member, Unit B', contrasts markedly from Unit A. The mean

grain sizes for samples from Unit B' are larger than those from Unit A, with a median of 602 μm (coarse sand; range from 253 to 961 μm, medium to coarse sand). The sediments in Unit B' are also better sorted than Unit A, ranging from 1.4 Φ to 2.3 Φ (well sorted to poorly sorted). Unit B, the transitional zone, falls between Unit A and Unit B granulometrically. It has grain sizes ranging from 193.2 to 811 μm (fine to coarse sand) and a median grain size of 335.7 μm (medium sand). Sorting is also intermediate between Unit A and Unit B, ranging from 1.6 to 4.1 Φ (moderately sorted to very poorly sorted).

Not only do the stratigraphic units contain distinct sedimentological character, but different geomorphic positions within the bar forms include unique granulometric signatures. For example, coarse sand and gravel (grains larger than 500 μm) and sorting (Φ) within the upper most unit of each bar form (Unit B') plot in a distinct field (Fig. 14B). The sediments from the core at the crest of the parabolic bar is dominated (85-95%) by sediments with grain size of larger than 500 μm (coarse sand and larger) and are typically moderately sorted (most fall between 1.7 Φ and 1.9 Φ) (Fig. 13). In contrast, sediments from the core on the flank of the parabolic bar form contain less than 55% grains larger than 500 μm and are less well-sorted, ranging from 1.9 Φ to 2.3 Φ (moderately to poorly sorted) (Fig. 12).

Similar to the relationship between sedimentological attributes and geomorphic position within parabolic bars, grain size and sorting vary with position in transverse shoulder bars (Fig. 15B). The cores reveal that sediments from the crest of the transverse shoulder bar consist of 80-95% of grains larger than 500 μm, with sorting between 1.7 Φ and 2.0 Φ (moderately sorted to poorly sorted). Comparatively, the sediment in cores from the transverse shoulder bar flank contain only 40-80% of grains larger than 500 μm with variable sorting, ranging from 1.4 Φ (well sorted) to 2.2 Φ (poorly sorted) (Fig. 9).

At a larger scale, within the oolitic sand of Unit B', the granulometric signature of sediments from the crests of transverse shoulder bars are broadly similar to those on the crests of parabolic bars (Fig. 15B). These sediments plot in a well-defined field. In contrast, the ooid-rich sediments from the flanks (but still in Unit B') include distinct signatures in the parabolic bar and the transverse shoulder bar.

Sediments from the flank of the parabolic bar are generally finer and less well sorted than transverse shoulder bar flank sediments.

DISCUSSION

Large-Scale Evolution

The stratigraphic record represents the archive of the history of Earth surface systems through time. Throughout geologic history, carbonate systems are characterized by a pronounced variability, in large part related to changing biota (James, 1984; Schlager, 2000). Ooid sands are unique in that they are one class of carbonate sedimentologic systems occurring throughout geologic time (Evans, 1984; Cantrell and Walker, 1985; Handford, 1988; Sumner and Grotzinger; 1993; Rankey et al., 2006; Reeder and Rankey, 2008; Rankey and Reeder, 2011). Likewise, beyond their importance as paleoclimatic, paleoceanographic, and paleodepositional indicators (Mackenzie and Pigott, 1981; Sandberg, 1983; Wilkinson et al., 1985; Opdyke and Wilkinson, 1993), these bodies are important hydrocarbon and water reservoirs in many basins across the world (Todd, 1976; Davies et al., 2000; Harris, 2010).

The primary means of understanding stratigraphy is by examining spatial and vertical patterns in sedimentologic character (grains, textures, sedimentary structures). Although an important avenue of research is careful examination of patterns in ancient oolitic systems (Todd, 1976; Handford, 1988; Burchette et al., 1990; Keith and Zuppann, 1993; Palermo et al., 2010), to better understand the history recorded by ooid shoals, numerous researchers have examined Holocene oolitic shoals (Purdy, 1961; Ball, 1967; Hine, 1977; Harris, 1979; Rankey et al., 2006) as analogs for ancient systems. This approach provides the unique opportunity to examine, quantify and relate sedimentologic processes to spatial variability in granulometric character of surface sediments (Purdy, 1961; Ball, 1967; Gonzalez and Eberli, 1997; Rankey et al., 2006; Reeder and Rankey, 2008). A logical next step, however, is explicitly linking these processes and spatial patterns observed in recent shoals with the stratigraphic record that they have produced.

In this context, Lily Bank represents a well-studied Holocene ooid shoal. Several studies (Hine, 1977; Rankey et al., 2006; Rankey and Reeder, 2011) have described both oceanographic processes and surficial sedimentologic products in this area. Integration of these insights with seismic and core data that capture the geologic record of the shoal suggest that Lily Bank is not a static system, unchanging through time. Instead, both the core and seismic data reveal several distinct units and a complex stratigraphic evolution.

In the focus area on Lily Bank, for example, Unit Z, the unit just above a gently seaward-dipping Pleistocene bedrock, varies in thickness (Figs. 4, 5, 14). Although it was not cored and its sedimentology is unknown, this unit is interpreted as a basal transgressive deposit representing earlier Holocene platform flooding. The overlying unit, Unit A, is up to 5.8 m thick, and consists of a poorly sorted gravelly muddy sand with few to no ooids that forms a sheet-like deposit across the area (Figs. 4, 5, 6D, 7-13). Based on the relatively high mud content, open marine fauna, and lack of ooids, this unit is interpreted to represent a lagoonal, low-energy environment (Fig. 14) not unlike areas platformward of the present-day shoal complex today. A faint reflector, Reflector B, separates Unit A from Unit B (Figs. 4-6). Unit B is a thinner (< 4.2 m) unit that includes an upward increase in abundance of ooids. It includes less mud and is better sorted than the underlying unit (Figs. 7-14). On the basis of the decrease in mud and trends in ooid abundance, Unit B is interpreted to represent channels and bar-flank areas that gradually shallowed, related to the approach of nearby bar forms or the shoal as a whole (Fig. 14C,D). This unit forms the uppermost deposit in present-day channels. The active bar forms are capped by Unit B' (Fig. 4; Fig. 5; Fig. 6C; Fig. 6F). This uppermost unit reaches up to 3.8 m thick, and includes moderately to well-sorted ooid sand with high-amplitude shingled reflectors in the seismic data (Fig. 4; Fig. 5; Fig. 6F; Fig. 14). This uppermost unit is interpreted to represent the stratigraphic record of the high-energy ooid shoal.

Collectively, these stratigraphic elements reveal the details of the large-scale geologic evolution of Lily Bank in this area, which is consistent with the conceptual model of Hine (1977). This model suggests that following initial flooding in the Holocene (Figure 16A), Lily Bank initiated downdip,

related to the location of narrow re-entrants at the bank margin. These openings between the reefs funneled flow, increasing energy, generating linear, flow-parallel tidal sand ridges ~7 km onto the platform (Fig. 16B). As Holocene sea level continued to rise, the active shoal migrated platformward to its present location, where individual bar forms are characterized by net platformward transport even today (Hine, 1977; Rankey et al. 2006). Under the presently active Lily Bank, however, the abundance of fines, peloids, and the absence of ooids in the lower unit (Unit A) suggest that initial deposition there was under relatively low-energy conditions (Fig. 16B). The transitional unit in the cores, which include variable granulometry and upward increases in ooid abundance (Fig. 16C), is interpreted to reflect net platformward migration. As the active shoal migrated platformward, the formerly active downdip tidal sand ridges became stabilized by sea grass (Fig. 16C).

Several attributes of the patterns of large-scale Holocene stratigraphic and geomorphic evolution of Lily Bank contrast with conceptual models for the stratigraphy of ooid shoals derived from other areas (e.g., Purdy, 1961; Harris, 1979; Evans, 1984). Numerous studies have suggested that the occurrence of ooid shoals is favored where a marked topographic high is found at, or near, the bank margin. In other words, a pre-existing bedrock high is an element necessary for the nucleation of shoals. This concept is consistent with the observation that ooid shoals require elevated flow speeds, which, in this model, is created by vertical restriction from the non-erodable bedrock. This concept has been applied to explain Holocene shoals near Joulter Cays (Harris, 1979) and Cat Cay (Purdy, 1961) on Great Bahama Bank and the Pleistocene Miami Oolite (Evans, 1984), each of which has been interpreted or observed to include bedrock surface with several meters of relief. In stark contrast to this conceptual model, however, the present-day active Lily Bank is floored by a gently seaward-dipping top-Pleistocene bedrock surface, with no marked topographic high that could represent the "bump." Thus, this shoal demonstrates that a marked pre-existing bedrock topographic high is not a condition necessary for the occurrence of an ooid shoal (Hine, 1977).

Nonetheless, the seismic and core data suggest the presence of topography at the top of Unit A, just under the oolitic unit. At this stratigraphic marker, there appears to be ~4 m of total relief across the area. This horizon includes lows that generally correspond to the positions of channels between bars, and highs underlying bar forms, with ~1-1.5 m relief across any one bar form. Although this horizon includes changes in elevation, cores from highs and lows include no marked sedimentologic differences within Unit A. Thus, it remains unclear the factors that controlled the depositional topography within this unit. It is clear, however, that these syndepositional topographic highs and lows are broadly comparable to the present-day bar form topography (Fig. 4; Fig. 5; Fig. 14).

The evolution of Lily Bank provides an alternative to the model that shoals are dominantly oceanward-prograding systems (although many are; Purdy, 1961; Harris, 1979; Burchette et al., 1990). As discussed above, the sedimentology and stratigraphy illustrate that Lily Bank as a whole has stepped platformward more than 10 km in the Holocene (Hine, 1977; Fig. 16). Nonetheless, at the scale of individual bar forms, migration can be driven by on-bank transport (as seen by the transverse shoulder bars and flood-oriented parabolic bars), or off-bank transport (evident in the ebb-oriented parabolic bars). Thus, although Lily Bank has complimentary flood- and ebb-migrating bar forms at the small scale, the shoal-scale direction of migration is platformward.

Bar-Scale Evolution and Sedimentology

At a finer scale, patterns within individual bar forms illustrate complex dynamics. In this tidal shoal, although the net transport is platformward, individual bar forms are strongly influenced by the detailed patterns of both ebb and flood tides (Rankey et al., 2006; Rankey and Reeder, 2011). As a result, bar forms include a mix of orientations, some of which have been interpreted to be migrating oceanward, and others moving platformward (Rankey et al., 2006). Within these bar forms, shingled geometries of reflectors in the upper oolitic unit (Unit B') on the seismic data, and dipping strata in the cores, reflect trends in bedform migration. In these, parabolic bars that appear flood-dominated based on their surficial

geomorphic character (parabola apex to the south) are clearly prograding platformward, whereas the ebb-dominated parabolic bars (apex to the north) have net oceanward transport. These patterns are broadly consistent with the general conceptual model suggested by Rankey et al. (2006).

The facies succession present in bars on Lily Bank contrasts with patterns documented in other ooid shoals. For example, Purdy (1961) generalizes the stratigraphic succession at Cat Cay as a thick (~3 m) ooid sand sharply overlying the Pleistocene bedrock. Likewise, a typical succession at Joulter Cays (Harris, 1979; Grammer et al., 2004) includes a basal transgressive lithoclastic sand, that passes up into a muddy fine peloidal sand and finally a capping muddy ooid sand. Clean, well sorted ooid sand is present only on the seaward flank of the shoal complex. In contrast, Lily Bank contains a more heterogeneous stratigraphic framework. In its lower part, overlying Pleistocene bedrock, includes up to ~6 m of poorly sorted gravelly muddy sand commonly with >25% very fine sand and mud (< 125 μm) and few ooids. This lower unit, the thickest in the succession, is sharply overlain by a more well sorted sand with upward increasing ooid abundances and decreasing fines (< 125 μm fraction is commonly < 5%) up to ~5 m thick. This deposit is interpreted as progradational deposits, representing ooids shed off the front of the bar forms approaching the area and finally the well-sorted oolitic sand, representing the active ooid shoal - Lily Bank. Thus, ooid shoals need not be thick, homogenous clean ooid-dominated sand, from bedrock to the surface.

Within the shoal complex, each unit (A, B, B') includes several granulometrically distinct units (Figure 15A). Similarly, even within oolitic-dominated sediment, sand from the bar crests is coarser and better sorted than that from the flanks of bar forms (Figure 15B). These observations confirm the general observation of the close relation between geomorphology and sedimentology in ooid shoals (Rankey et al., 2006; Reeder and Rankey, 2008; Rankey and Reeder, 2011). Nonetheless, there is variability within this framework. For example, the sediments from Unit B' from a core on the flank of the transverse shoulder bar (Fig. 3) include a finer and less well-sorted lower unit and a coarser and better sorted upper unit that includes sediments similar to sediments found on the crest of a transverse shoulder bar. This

pattern is interpreted to reflect incipiently changing morphology, from a transverse shoulder bar crest to a parabolic bar crest (Rankey et al., 2006). Sediments within the upper unit are reworked, and subjected to more bi-directional flow. These reworked sediments of the capping unit have elevated ooid abundance, are better sorted, and are trough cross-stratified, characteristics typical of a bar crest.

These trends collectively suggest that not only do surface sediments in the Lily Bank area vary based on geomorphic position (Rankey et al., 2006), the stratigraphic record from different positions is distinct. Although these observations represent data from only one shoal complex, if the linkage between bar form geomorphic position and sedimentological attributes is validated with further investigation, several important related implications for understanding and predicting trends in ancient analogs arise. For example, these relationships suggest that paleogeomorphic setting and configuration of ancient ooid shoals might be discerned based on limited data, such as careful granulometric analysis of one or two cores. Similarly, the close relationship between sediment granulometry and bar position emphasizes the close linkages between geomorphic position and depositional porosity and permeability. Although the ultimate character of porosity and permeability is complicated in carbonate strata due to intraparticle porosity and diagenetic influences, these results suggest that geomorphic bodies (and potential reservoir bodies) may include systematic variability in original porosity and permeability, which may ultimately impact diagenetic trends.

CONCLUSIONS

Carbonate successions contain multi-scale heterogeneity and a complex stratigraphic record as a product of diverse processes. To better understand the potential complexity of ooid shoals, a stratigraphically important facies, this study explores the sedimentology and stratigraphy of Lily Bank, an active Holocene ooid shoal. Analysis of shallow seismic and core data reveal that the stratigraphic succession of Lily Bank, above relatively flat Pleistocene bedrock, includes a basal transgressive unit with variable thickness. Overlying this basal deposit is a sheet-like unit with a seismically transparent signature

of up to 6 m of poorly sorted gravelly muddy sand with few to no ooids and an abundance of fines (Unit A). A sharp contact (Reflector B) marks the base of a transitional zone, characterized by an increase in ooids, less abundant fines, increased mean grain size, and better sorting. This transition zone gradually passes through a reflector (Reflector B') to the uppermost unit. This uppermost unit, Unit B', is generally a well-sorted, coarse grained, ooid-dominated sand. The three main stratigraphic units (Units A, B, and B') have distinct ranges of grain sizes and sorting. Unit A generally contains fine sand that is poorly sorted while Unit B' has medium to coarse sand that is well-sorted. Unit B, the transitional unit, falls in between Units A and B'. This stratigraphic complexity offers an alternative conceptual model to other ooid shoals that include thick Holocene oolitic sand accumulations or clean oolitic sand only on their margins.

Lily Bank, the active ooid shoal, initiated in a downdip, more marginward position in the earlier Holocene and has subsequently backstepped over ~ 2.5 km. Regionally, the Pleistocene supporting Lily Bank is gently dipping oceanward and has no significant underlying topographic "bump" (cf. Purdy, 1961). Instead, it appears that topography formed during the Holocene and hydrodynamics have influenced the location of the shoal complex.

At a finer scale, the results illustrate a close linkage between geomorphic position and sediment size, sorting, and type. If these results are validated by similar results elsewhere, they suggest that geomorphic position and laterally adjacent facies might be predicted from sedimentologic variability. Similarly, it illustrates a close relationship between potential reservoir bodies and their (depositional) porosity and permeability attributes.

WORKS CITED

Ball, M.M., 1967, Carbonate sand bodies of Florida and the Bahamas: *Journal of Sedimentary Petrology*, v. 37, p. 556-591.

Blott, S.J., and Pye, K., 2001, Gradistat: A grain size distribution and statistics package for the analysis of unconsolidated sediments: *Earth Surface Processes and Landforms*, v. 26, p. 1237-1248.

Burchette, T.P., Wright, V.P., and Faulkner, T.J., 1990, Oolitic sand body depositional models and geometries, Mississippian of southwest Britain: Implications for petroleum exploration in carbonate ramp settings: *Sedimentary Geology,* v. 68, p. 87-115.

Cantrell D., and Walker, K., 1985, Depositional and diagenetic patterns, ancient oolite: Middle Ordovician, Eastern Tennessee: *Journal of Sedimentary Petrology*, v. 55, p. 518-531.

Davies, R., Hollis, C., Bishop, C., Gaur, R., and Haider, A.A., 2000, Reservoir geology of the Middle Minagish Member (Minagish Oolite), Umm Gudair Field, Kuwait: *Middle East Models of Jurassic/Cretaceous Carbonate Systems*, (SEPM Special Publication), v. 69, p. 273-286.

Enos, P., 1977, Quaternary depositional framework in South Florida, part I: Holocene sediment accumulations of the South Florida shelf margin: *Geological Society of America Memoir* 147, p. 1-130

Evans, C., 1984, Development of an ooid sand shoal complex: The importance of antecedent and syndepositional topography: *SEPM Core Workshop,* v. 5, p. 392-428.

Folk, R.L., 1954, The distinction between grain size and mineral composition in sedimentary rock nomenclature: *Journal of Geology*, v. 62, p. 344-359.

Folk, R.L., and Ward, W.C., 1957, Brazos River bar: A study of significance of grain size parameters: *Journal of Sedimentary Petrology*, v. 27, p. 3-26.

Ginsburg, R.N., 1956, Grain size of Florida carbonate sediments: *American Association of Petroleum Geologists Bulletin,* v. 40, p. 2384-2427.

Gonzalez, R., and Eberli, G.P., 1997, Sediment transport and bedforms in a carbonate tidal inlet: Lee Stocking Island, Exumas, Bahamas: *Sedimentology*, v. 44, p. 1015-1030.

Handford, R., 1988, Review of carbonate sand-belt deposition of ooid grainstones and application to Mississippian reservoir, Damme Field, Southwestern Kansas: *American Association of Petroleum Geologists Bulletin*, v. 72, p. 1184-1199.

Harris, P.M., 1979, Facies anatomy and diagenesis of a Bahamian Ooid Shoal: *Sedimenta VII: Comparative Sedimentology Lab,* University of Miami, Miami, 163 pp.

Harris, P.M. and Vlaswinkel, B.M., 2008, Modern isolated carbonate platforms: Templates for quantifying facies attributes of hydrocarbon reservoirs, *in* Lukasik, J. and Simo, T., eds., Controls on Carbonate Platform and Reef Development: *SEPM Special Publication 89,* p. 323-341.

Harris, P.M, and Ellis, J.M., 2009, Satellite imagery, visualization, and geological interpretation of the Exumas, Great Bahama Bank - An analog for carbonate sand reservoirs: *SEPM Short Course Notes 53*, p. 1-49 (2 DVDs).

Harris, P.M., 2010, Delineating and quantifying depositional facies patterns in carbonate reservoirs: insight from modern analogs: *American Association of Petroleum Geologists Bulletin*, v. 94, p. 61-86.

Hine A., 1977, Lily Bank, Bahamas: history of an active oolite sand shoal: *Journal of Sedimentary Petrology*, v. 47, p. 1554-1581.

Jackson, P.T., 1995, The sedimentology and Holocene evolution of the Caicos Cays, Turks and Caicos Islands, British West Indies: *Unpublished M.Sc. Thesis,* University of Calgary.

James, N.P., 1984, Reefs, *in* Walker, R.G., ed., Facies Models: Geological Society of Canada, p. 229-244.

Incze, M.L., 1998, Petrophysical properties of shallow-water carbonates in modern depositional and shallow sub-surface: *Unpublished Ph.D. Dissertation,* University of Miami, Coral Gables, FL, 405 pp.

Keith, B.D., and Zuppann, C.W., eds., 1993, Mississippian Oolites and Modern Analogs: *American Association of Petroleum Geologists, Studies in Geology*, v. 35, 265 pp.

Mackenzie, F.T., and Pigott, J.D., 1981, Tectonic controls of Phanerozoic sedimentary rock cycling: *Geological Society of London Journal,* v. 138, p. 183-196.

Morgan, W.A., 2008, Holocene sediments of northern and western Caicos Platform, British West Indies: *SEPM Core Workshop 22*, p. 75-104.

Opdyke, B.N., and Wikinson, B.H., 1993, Carbonate mineral saturation state and cratonic limestone accumulation: *American Journal of Science*,v. 293, p. 217-234.

Palermo, D., Aigner, T., Nardon, S., and Blendinger, W., 2010, Three-dimensional facies modeling of carbonate sand bodies: Outcrop analog study in an epicontinental basin (Triassic, southwest Germany): *American Association of Petroleum Geologists Bulletin*, v. 94, p. 475-512.

Purdy, E.G., 1961, Bahamian oolite shoals, *in* Peterson, J.A. and Osmond, J.C., eds., Geometry of Sandstone Bodies: *American Association of Petroleum Geologists Special Publication 22*, p. 53-63.

Purkis, S.J., Reigl, B.M., and Andrefouet, S., 2005, Remote sensing of geomorphology and facies patters on a modern carbonate ramp (Arabian Gulf, Dubai, U.A.E.): *Journal of Sedimentary Research*, v. 75, p. 861-876.

Rankey E.C., Riegl B., and Steffen, K., 2006, Form, function and feedbacks in a tidally dominated ooid shoal, Bahamas: *Sedimentology*, v. 53, p. 1191-1210.

Rankey, E.C., Guidry, S.A., Reeder, S.L., and Guarin, H., 2009, Geomorphic and sedimentologic heterogeneity along a Holocene shelf margin: Caicos platform: *Journal of Sedimentary Research*, v. 79, p. 440-456.

Rankey, E.C., and Reeder, S.L., 2011, Holocene oolitic marine sand complexes of the Bahamas: *Journal of Sedimentary Research*, v. 81, p. 97-117.

Reeder, S.L., and Rankey, E.C., 2009, Controls on morphology and sedimentology of carbonate tidal deltas, Abacos, Bahamas: *Marine Geology*, v. 267, p. 141-155.

Sandberg, P.A., 1983, An oscillating trend in Phanerozoic in nonskeletal carbonate mineralogy: *Nature*, v. 305, p. 19-22.

Schlager, W., 2000, The future of applied sedimentary geology: *Journal of Sedimentary Research*, v. 70, p. 2-9.

Shinn, E.A., Lidz, B.H., and Holmes, C.W., 1990, High-energy carbonate sand accumulation, the Quicksands, southwest Florida Keys: *Journal of Sedimentary Petrology*, v. 60, p. 952-967.

Sumner, D.Y., and Grotzinger, J.P., 1993, Numerical modeling of ooid size and the problem of Neoproterozoic giant ooids: *Journal of Sedimentary Petrology*, v. 63, p. 974-982.

Todd, R.G., 1976, Oolite-bar progradation, San Andres Formation, Midland Basin, Texas: *American Association of Petroleum Geologists Bulletin*, v. 60, p. 907-925.

Wanless, H.R., Tedesco, L.P. and Tyrrell, K.M., 1988, Production of subtidal tubular and surficial tempestites by Hurricane Kate, Caicos Platform, British West Indies: *Journal of Sedimentary Petrology*, v. 58, p. 739-750.

Wentworth, C.K., 1922, A scale of grade and class terms for clastic sediments: *The Journal of Geology*, v. 30, p. 377-392.

Wilkinson, B.H., Owen, R.M., and Carroll, A.R., 1985, Submarine hydrothermal weathering, global eustacy, and carbonate polymorphism in Phanerozoic marine oolites: *Journal of Sedimentary Petrology*, v. 55, p. 171-183.

Wilson, J.L., 1975, Carbonate Facies in Geologic History: New York, Springer-Verlag, 471 pp.

FIGURE CAPTIONS

Fig. 1 – Remote sensing images of the general Lily Bank study area on Little Bahama Bank (LBB) and Lily Bank area (LANDSAT data; highlighted by yellow box in the inset). Inset MODIS image shows the location on LBB. The focus area of Lily Bank is indicated by the yellow box. Note difference between the active Lily Bank (white in this image) and relict tidal sand ridges (previously active, now stabilized by sea grass) and the downdip Matanilla reefs.

Fig. 2 – Remote sensing image of Lily Bank, illustrating distinct barform morphologic end-members: transverse shoulder bars (red box) and parabolic bars (yellow box). Note the difference between straight crests of transverse shoulder bars, oriented roughly normal to on-bank flow, and the sinuous crests of parabolic bars that include distinct flood and ebb conduits. Image also shows subaqueous dunes on the crests of bar forms. Image copyright GeoEye.com.

Fig. 3 – Locations of seismic lines (red/yellow) and cores (black/blue) analyzed in this thesis. Illustrative seismic lines (yellow, Fig. 4, Fig. 5) and cores (blue dots, Figs. 7-9; 11-13) examined in greater detail in this thesis are highlighted. Seismic lines and cores were strategically located to capture the range of variability in bar forms, to explore sedimentological variability within and among the different bar forms.

Fig. 4 - Illustrative seismic line through a transverse shoulder bar; see Fig. 3 for location. A) Uninterpreted seismic line. B) Interpreted line indicating reflectors, seismic packages and coring locations. Note that the continuous Reflector Z, interpreted as Top Pleistocene, includes no pronounced high. Also note the local convergence of Reflector A with Reflector Z. Reflector B includes several m of relief, and Reflector B' is present only under the bar forms.

Fig. 5 - Illustrative seismic line through a parabolic bar; see Fig. 3 for location. Dominant (flood) tide here is from N to S. A) Uninterpreted seismic line. The sea-floor multiple is indicated. B) Interpreted seismic line. Note Reflector Z, interpreted as Top Pleistocene, has little topography and is continuous across the area. The overlying reflector, Reflector A', also has an irregular topography. Reflector B' occurs under bar forms, but is coincident with channel depths between bar forms and the lagoon. Coring locations also noted. C) Detail of interpreted line in the area of a parabolic bar crest. In this line, the shingled, moderate- to high-amplitude reflectors of Unit B' are evident, and indicate dip to the south.

Fig. 6 – Trends in depth of seismic horizons and thickness of seismic-defined units. A) Reflector Z depth. The reflector is shallowest under the southwestern transverse shoulder bar and deepest to the northeast and under the parabolic bars, with an overall gentle oceanward dip. B) Reflector B depth. Reflector B is shallowest under the southwestern transverse shoulder bar and deepens to the northeast. C) Depth of Reflector B'. Reflector B' is only evident under the active bar forms. Reflector B' shallows to the south both regionally and locally under each bar form. D) Unit A thickness. This unit is thickest under the active shoal, especially under the parabolic bars, and thins lagoonward. E) Thickness between reflectors B and B' (lower part of unit B). This unit is thickest away from the crests in the inter-bar channel and lagoon, whereas it thins under the crest of each bar form. F) Unit B' thickness; this unit is thicker under the active bar forms and thins away from the crests, and is generally thicker in the transverse shoulder bars than in the parabolic bars. Note that it is absent in the inter-bar channel and in the lagoon. Some

lines have been omitted based on low confidence (e.g., poor imaging or the dominance of a multiple obscuring the horizon) or ambiguous interpretations.

Fig. 7 – Sedimentological attributes from the lagoonal core (LBR 3.4). Note the lack of ooids, the highly mixed granulometry, and the overall upwards increase in mud content. In this and all following core data figures, note that the granulometry data are plotted with two axes – an upper axis for sand content that ranges from 80-100%, and a lower axis for gravel and mud content, which ranges from 0-20%.

Fig. 8 – Sedimentological attributes from the inter-bar channel core (LBR 1.4). Note the coarse lag at the base, passing to a lower unit with very few ooids and variable amounts of sand, mud, and gravel sized grains. Ooid abundance increases upwards in the Upper Unit while the granulometry remains variable. Refer to Fig. 7 for key.

Fig. 9 – Sedimentological attributes from the core from the flank of a transverse shoulder bar (LBR 1.3). The core includes three distinct units: a lower unit, a transitional unit, and an upper unit. Similar to the inter-bar channel, the base of the core contains a basal lag, and an ooid-poor lower unit. These are overlain by a transitional unit with a marked upwards increase in ooid abundance and sand content, with less mud and gravel. The upper unit is dominated by ooids and is comprised almost entirely of sand-sized grains with little to no mud and gravel. The upper unit can be further broken into two "subunits" based on distinct granulometric properties and changes in grain types (separated by the dashed grey line). Refer to Fig. 7 for key.

Fig. 10 – Representative thin sections from cores. A-C from a transverse shoulder bar core, D-F from a parabolic bar core. All photos have a scale of 500 μm. A) Base of lower unit that includes large intraclasts, *Halimeda*, and poor sorting. B) Top of lower unit, with a decrease in size and abundance of intraclasts and *Halimeda*, and the subtle increase in ooid abundance. C) Upper unit. Notice the abundance and size of ooids in this moderately sorted sand. D) Base of lower unit with large skeletal fragments, intraclasts, and few ooids. E) Top of lower unit, including a subtle increase in ooid abundance and smaller and fewer skeletal fragments and intraclasts. F) Upper unit. The sediments here are dominated by large, well-preserved ooids with some peloids and skeletal fragments.

Fig. 11 - Sedimentological attributes of a core from the crest of a transverse shoulder bar (LBR 1.2). The base of the core is the top of the lower unit, which passes into the transitional unit and an upward increase in ooid abundance. This transitional unit passes into the upper unit, which is dominated by ooids and has increased gravel and basically no mud. The upper unit can be broken down into several "subunits" based on ooid abundance and granulometric properties. Refer to Fig. 7 for key.

Fig. 12 – Sedimentological attributes from a core on the parabolic bar flank (LBP 1.2). This core includes three sedimentologically distinct units: a lower unit, characterized by almost no ooids with some mud and gravel, a transitional unit with an increase in ooids and higher mud content, and an upper unit, dominated by ooids with very little mud and gravel. Refer to Fig. 7 for key.

Fig. 13 - Sedimentological attributes from a core on the parabolic bar crest (LBP 1.1). This core is dominated by ooids and is mostly sand with little mud and gravel. The granulometry changes very little

throughout the core. Failure to penetrate below 1.35 m depth during several attempts suggests the presence of a continuous hardground. Refer to Fig. 7 for key.

Fig. 14 - Sedimentologic and stratigraphic interpretation of Lily Bank, based on integration of seismic data and core characterization. The cross-section lines illustrate are from a transverse shoulder bar (Fig. 4) and a parabolic bar (Fig. 5). Refer to Fig. 3 for locations. A) Large-scale interpretation of the succession across two transverse shoulder bars. D) Large-scale interpretation of the succession along the axis of a parabolic bar. B) Detailed interpretation of the stratigraphy in a transverse shoulder bar. General granulometric properties in cores along these transects are illustrated. D) Details of the stratigraphy in the parabolic bars. Note that both areas include a broadly similar succession: a relatively flat to oceanward dipping Pleistocene bedrock overlain by a basal transgressive deposit. This transgressive deposit is overlain by poorly sorted, burrowed, gravelly muddy sand, representing lagoonal sediments. These sediments in turn are overlain sharply by a transitional unit, characterized by a decrease in mud and increase in ooid abundance upwards, to the capping, ooid-dominated, well-sorted sand. The contact between the transitional unit and the overlying ooid sand is interpreted to represent a facies transition, reflecting mixing of sand shed in front of the prograding bar forms and the channel deposits. As discussed in the text, this transition is interpreted to have an impedance contrast sufficient to form a reflector (B') evident in the seismic data.

Fig. 15 – Cross plots of sedimentological attributes among the stratigraphic units (Unit A and Unit B) and the bar form morphology (transverse shoulder bar and parabolic bar). A) Mean grain size versus sorting, illustrating the distinctions among the lower unit (Unit A) from the overlying oolitic unit (Unit B'), and the intermediate unit (Unit B) B) Fraction of sediment >500 μm versus sorting, limited to sediments within Unit B'. Each color-size pair represents a distinct geomorphic position along a bar form. The transverse shoulder bar flank is divided into upper and lower regions. The upper transverse shoulder bar flank based on its evolution from a transverse shoulder bar to a parabolic bar. The upper unit is subjected to an increased influence of the ebb-tide, reworking the sediments similarly to the processes on bar crests, and is therefore assumed to be crest sediments. The transverse shoulder bar flank lower unit was subjected to a dominant flood tide, and is therefore interpreted as flank sediments.

Fig. 16 – Interpreted large-scale Holocene evolution of Lily Bank, based on the observations of this study and Hine (1977). Study area indicated by red box. A) Early to Mid-Holocene. Little Bahama Bank was an exposed platform bordering the open ocean. B) Late Holocene, early rapid sea level rise and platform flooding. During this period, proto-Lily Bank included active downdip tidal sand ridges, and the study area was a lower-energy lagoonal setting (e.g., deposition of Unit A). C) Present. Note that the active shoal has backstepped, and downdip tidal sand ridges are stabilized.

FIGURES

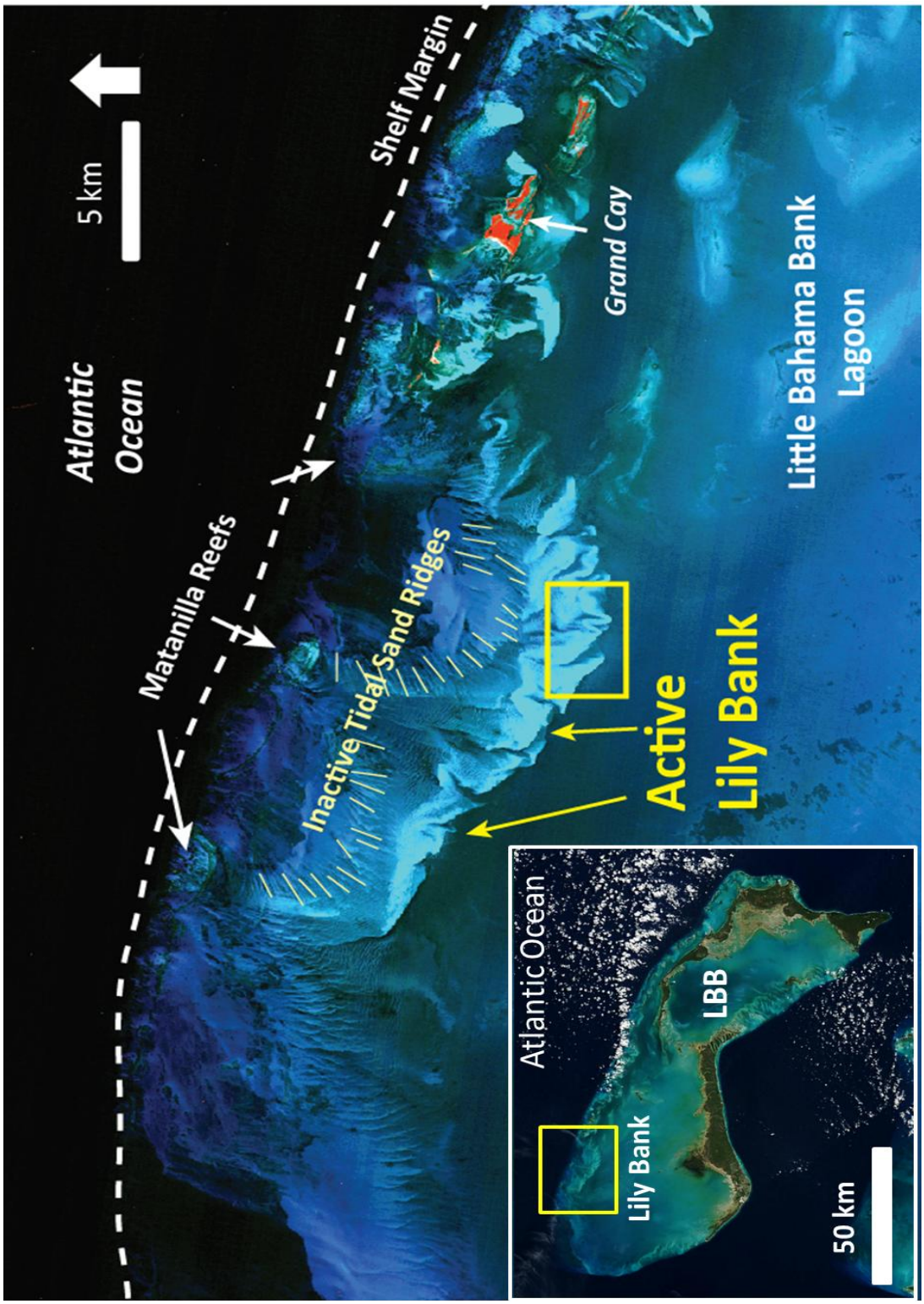

Fig. 1

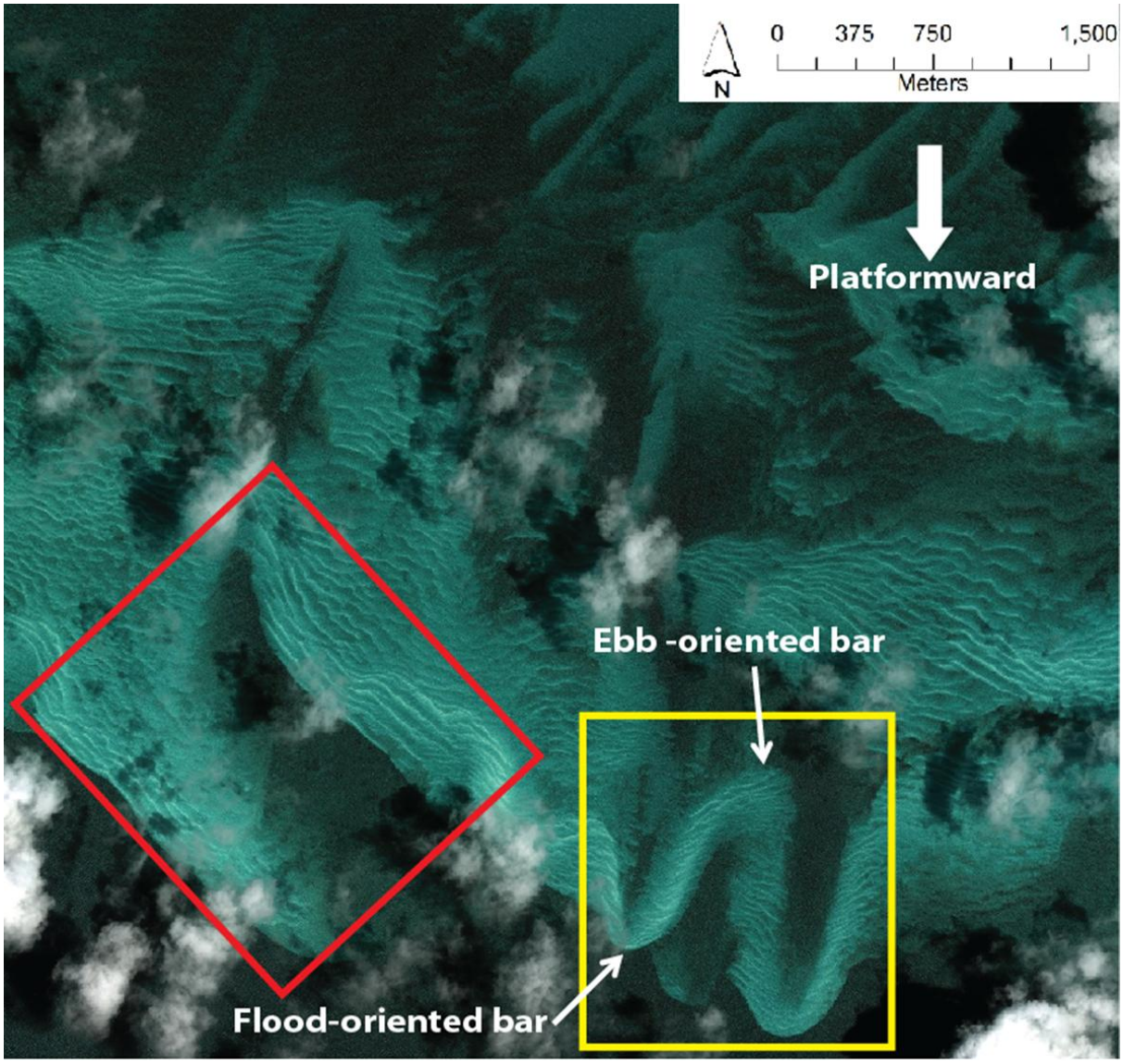
N
0
375
750
1,500
Meters
Platformward
Ebb -oriented bar
Flood-oriented bar

Fig. 2

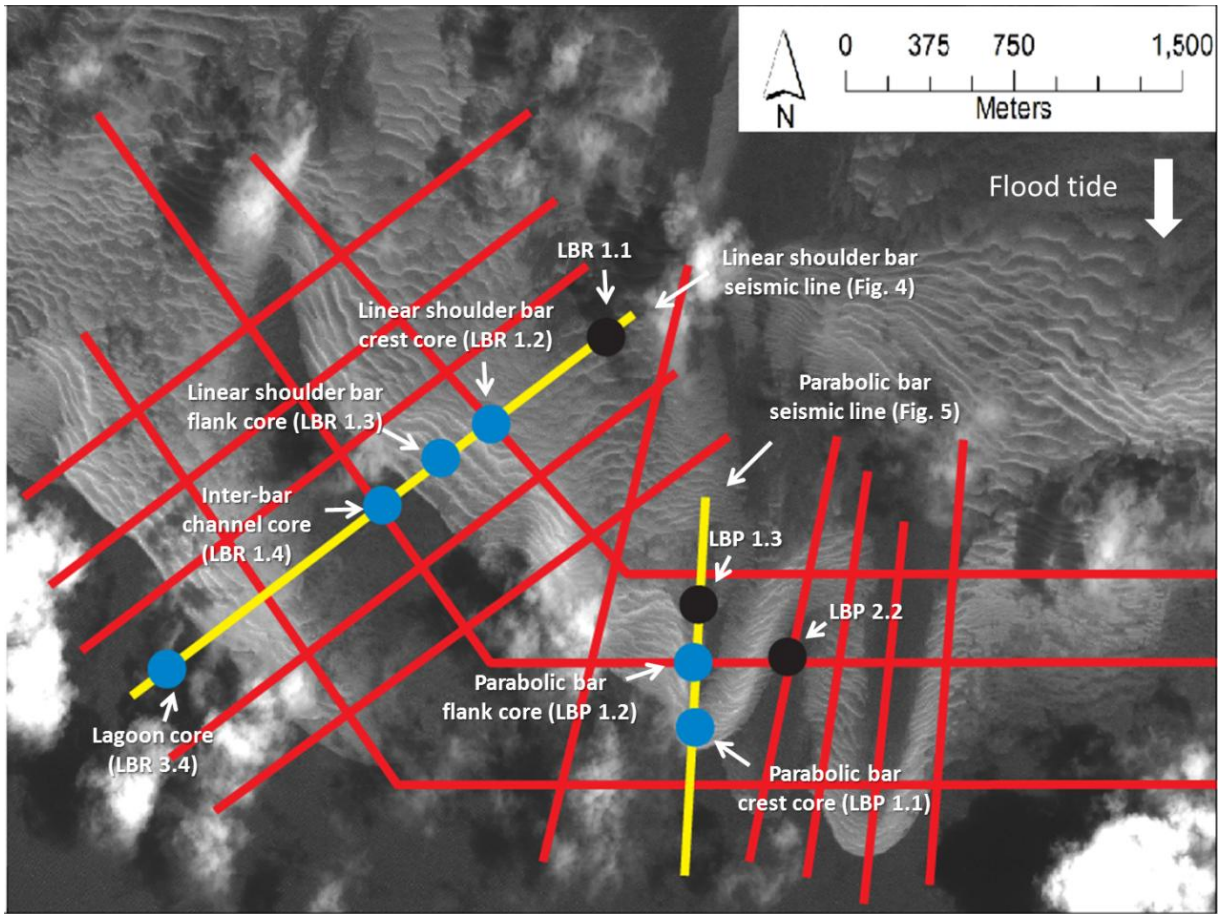
N
0
375
750
1,500
Meters
Flood tide
LBR 1.1
Linear shoulder bar seismic line (Fig. 4)
Linear shoulder bar crest core (LBR 1.2)
Linear shoulder bar flank core (LBR 1.3)
Parabolic bar seismic line (Fig. 5)
Inter-bar channel core (LBR 1.4)
LBP 1.3
LBP 2.2
Parabolic bar flank core (LBP 1.2)
Lagoon core (LBR 3.4)
Parabolic bar crest core (LBP 1.1)

Fig. 3

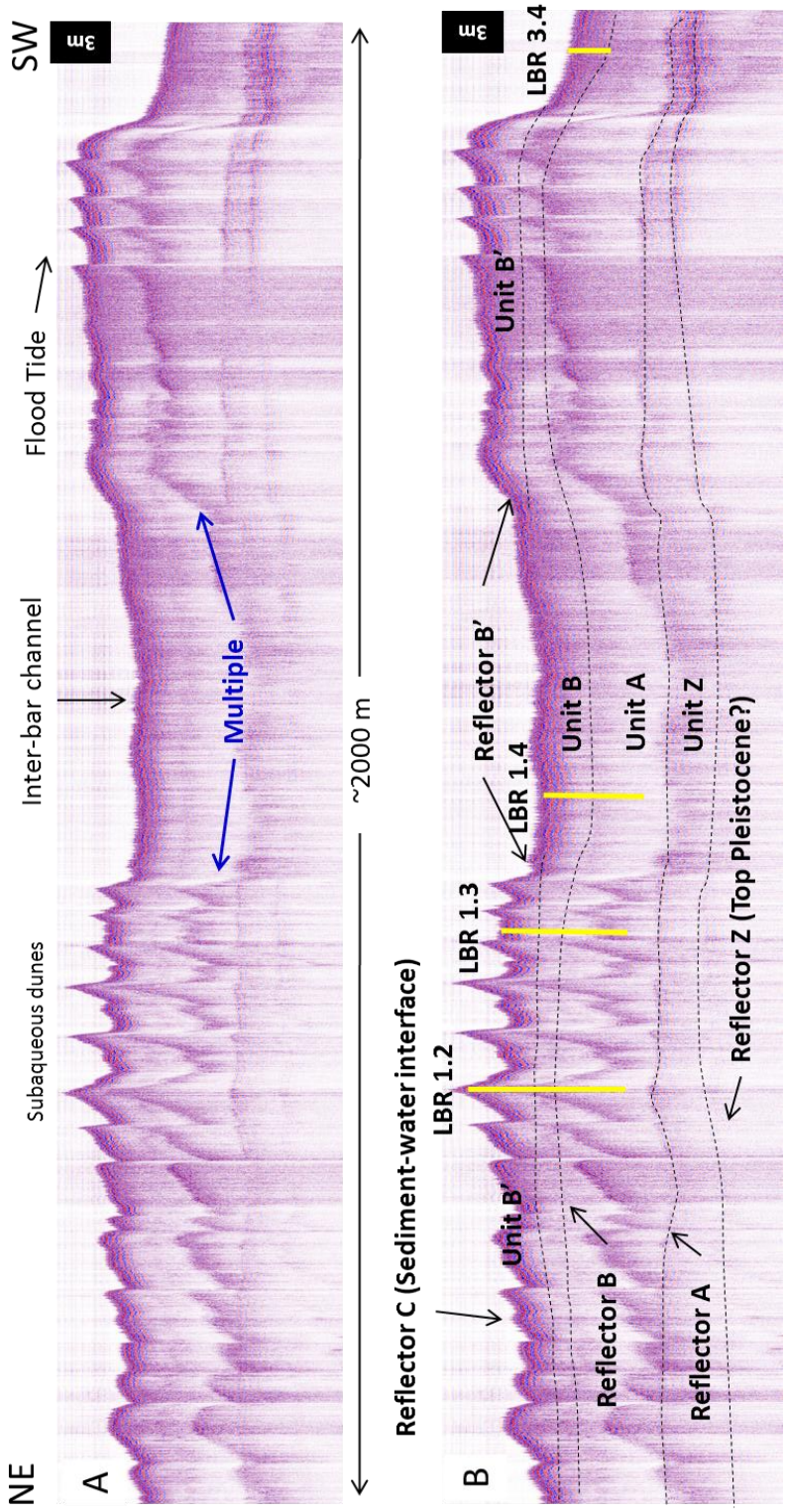
SW
NE
3m
3m
A
B
Flood Tide
Inter-bar channel
Subaqueous dunes
Multiple
~2000 m
Reflector C (Sediment-water interface)
LBR 1.2
LBR 1.3
LBR 1.4
Reflector B'
LBR 3.4
Unit B'
Unit B
Unit A
Unit Z
Unit B'
Reflector B
Reflector A
Reflector Z (Top Pleistocene?)

Fig. 4

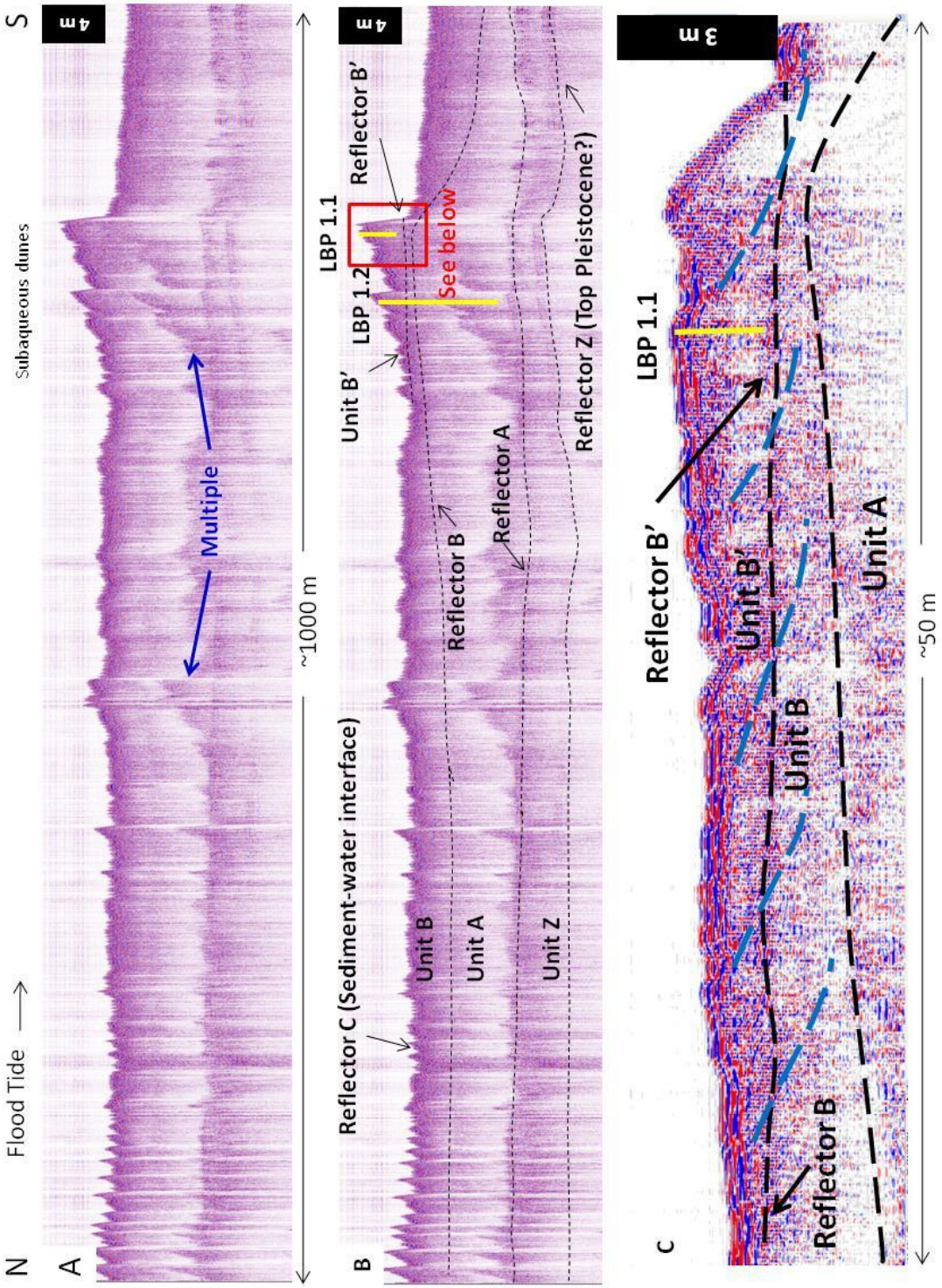
S
N
Flood Tide
Subaqueous dunes
A
4 m
Multiple
~1000 m
B
4 m
Reflector C (Sediment-water interface)
Unit B
Unit A
Unit Z
Reflector B
Reflector A
Reflector Z (Top Pleistocene?)
Unit B'
LBP 1.2
LBP 1.1
Reflector B'
See below
C
3 m
Reflector B'
LBP 1.1
Unit B'
Unit B
Unit A
Reflector B
~50 m

Fig. 5

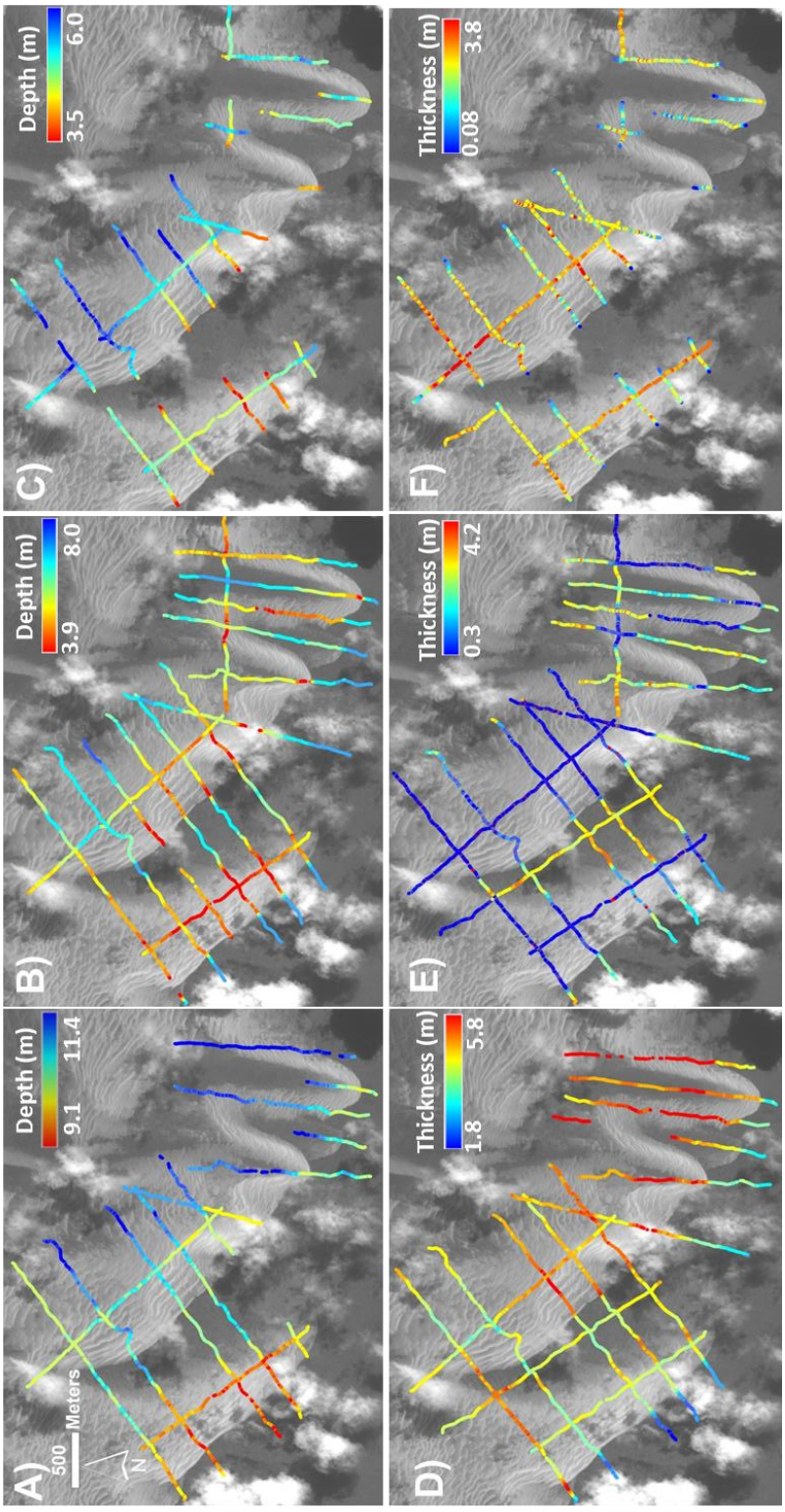
A)
Depth (m)
9.1
11.4
500
Meters
N
B)
Depth (m)
3.9
8.0
C)
Depth (m)
3.5
6.0
D)
Thickness (m)
1.8
5.8
E)
Thickness (m)
0.3
4.2
F)
Thickness (m)
0.08
3.8

Fig. 6

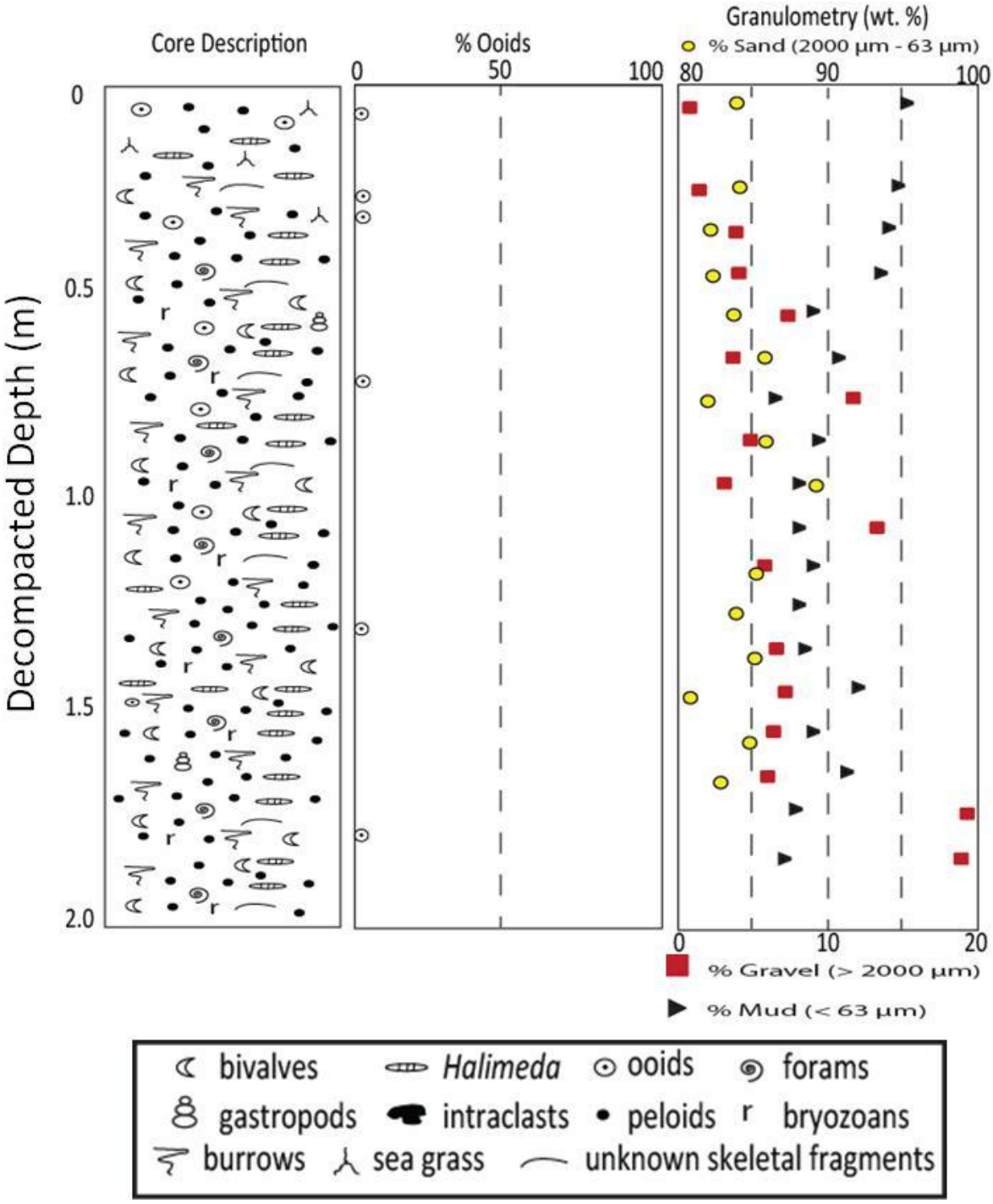
Core Description
% Ooids
Granulometry (wt. %)
% Sand (2000 µm - 63 µm)
Decompacted Depth (m)
0
0.5
1.0
1.5
2.0
0
50
100
80
90
100
0
10
20
% Gravel (> 2000 µm)
% Mud (< 63 µm)
bivalves
Halimeda
ooids
forams
gastropods
intraclasts
peloids
bryozoans
burrows
sea grass
unknown skeletal fragments

Fig. 7

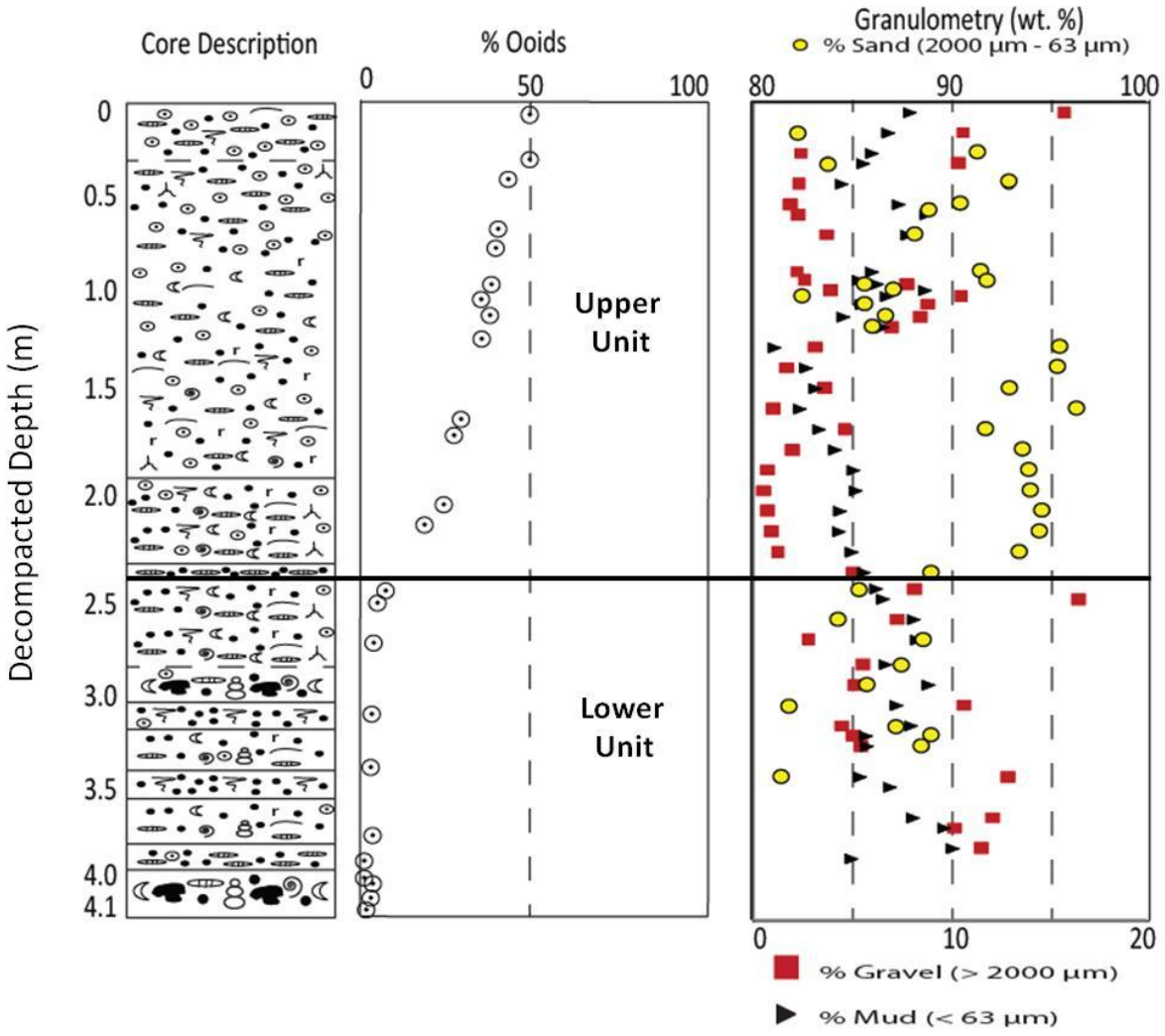
Core Description
% Ooids
Granulometry (wt. %)
% Sand (2000 µm - 63 µm)
Decompacted Depth (m)
0
0.5
1.0
1.5
2.0
2.5
3.0
3.5
4.0
4.1
0
50
100
80
90
100
Upper Unit
Lower Unit
0
10
20
% Gravel (> 2000 µm)
% Mud (< 63 µm)

Fig. 8

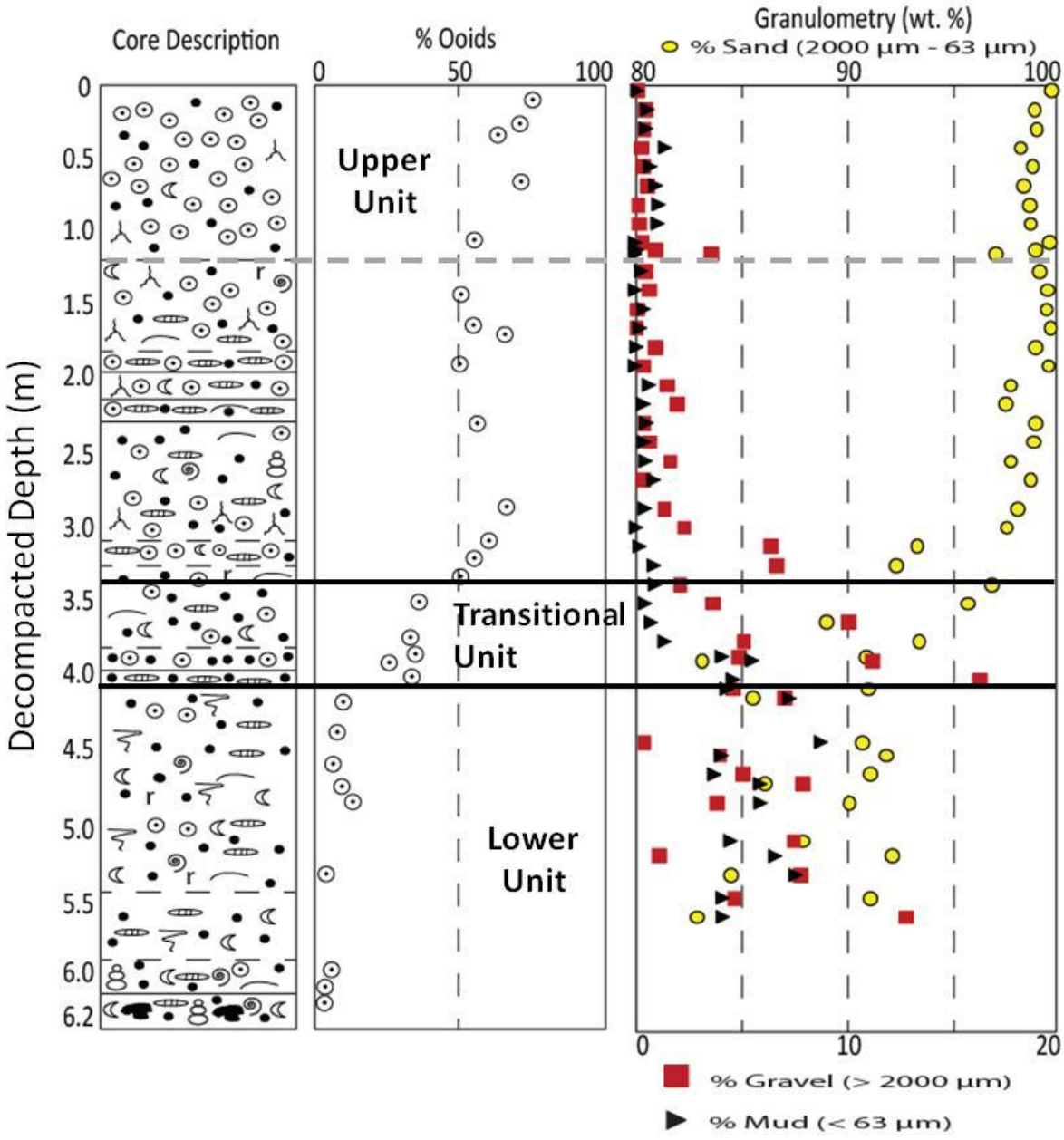
Core Description
% Ooids
0
50
100
Granulometry (wt. %)
% Sand (2000 µm - 63 µm)
80
90
100
Upper Unit
Transitional Unit
Lower Unit
Decompacted Depth (m)
0
0.5
1.0
1.5
2.0
2.5
3.0
3.5
4.0
4.5
5.0
5.5
6.0
6.2
0
10
20
% Gravel (> 2000 µm)
% Mud (< 63 µm)

Fig.9

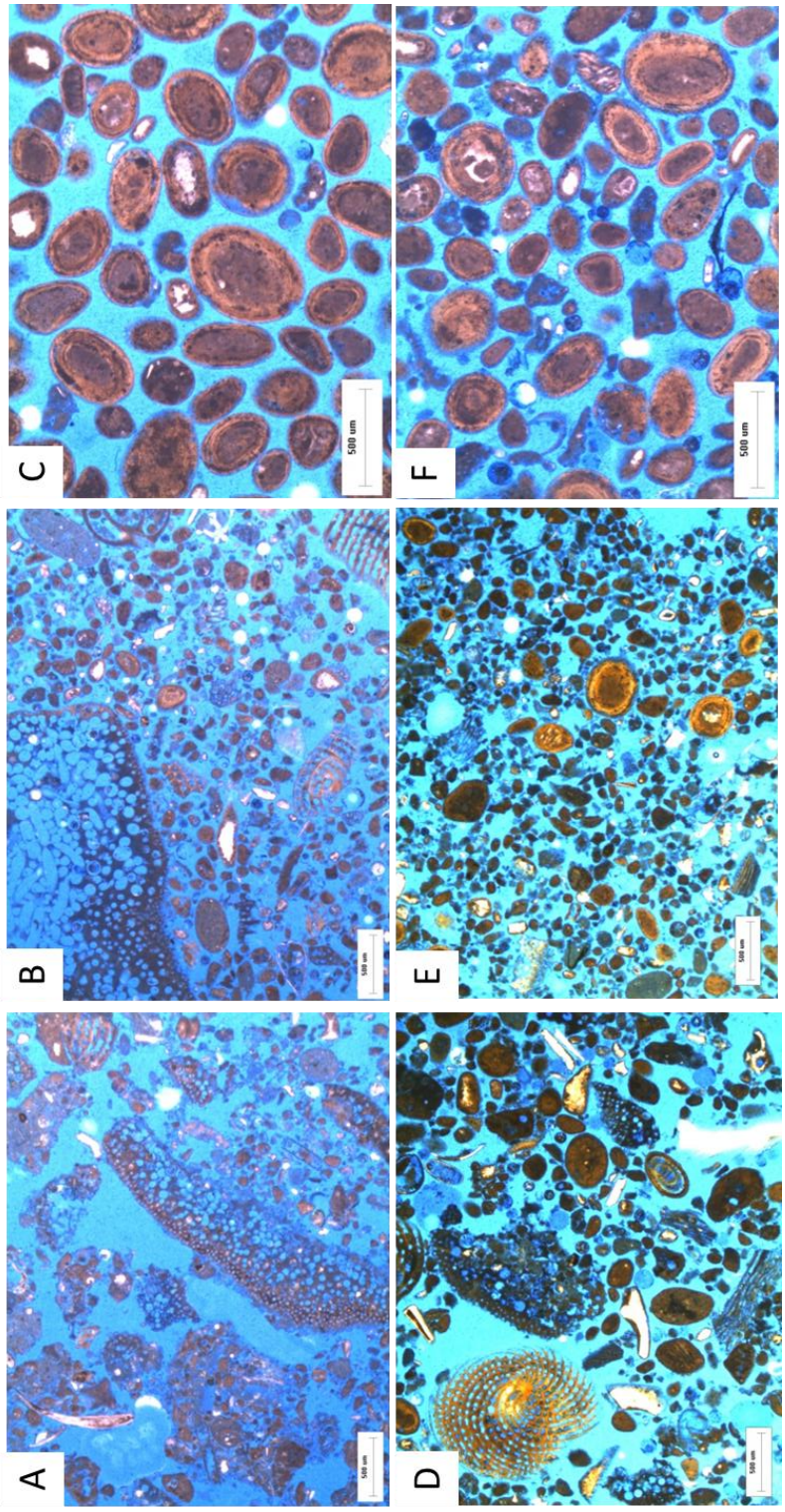

Fig. 10

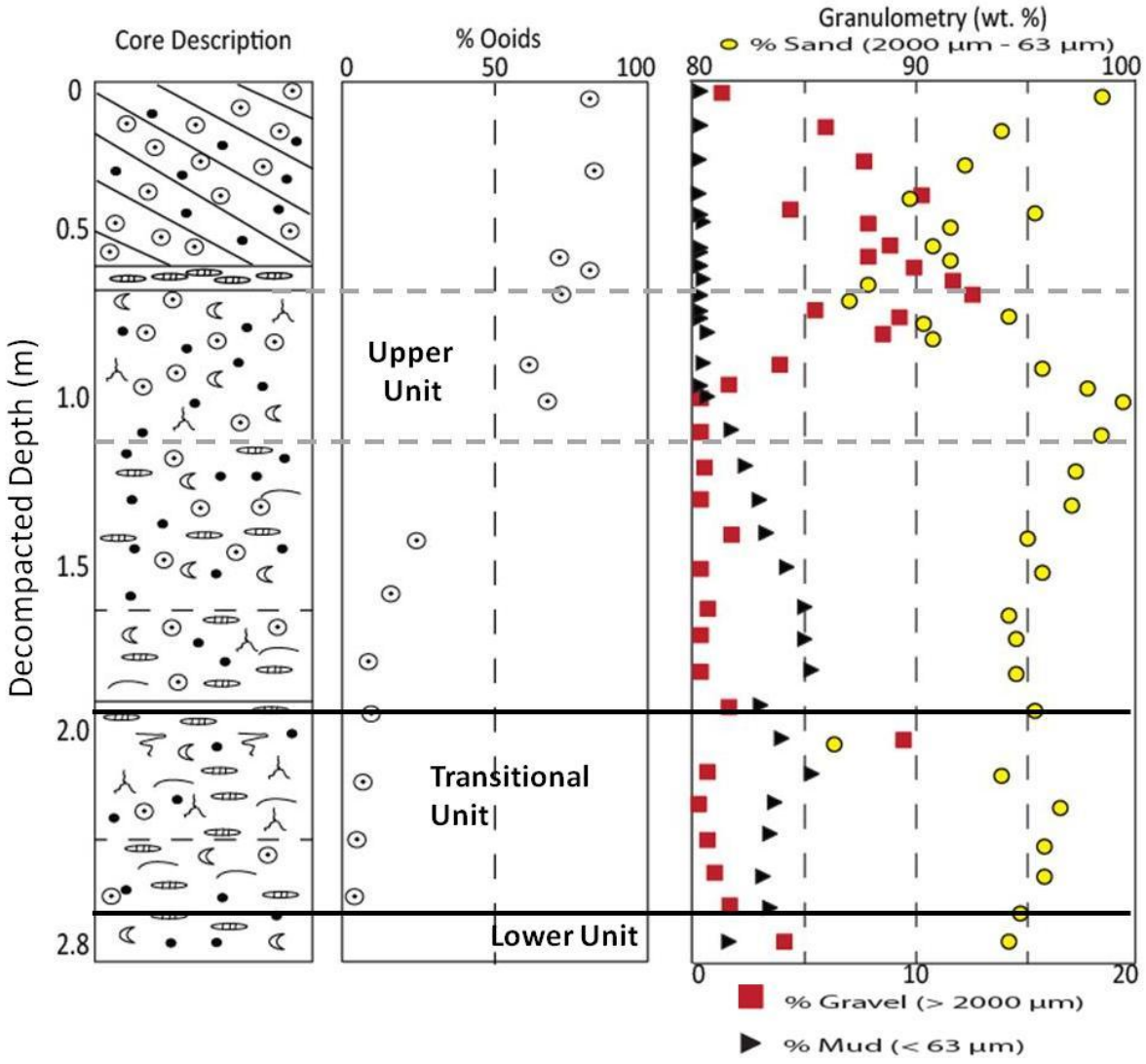
Core Description
% Ooids
0
50
100
Granulometry (wt. %)
% Sand (2000 µm - 63 µm)
80
90
100
Decompacted Depth (m)
0
0.5
1.0
1.5
2.0
2.8
Upper Unit
Transitional Unit
Lower Unit
0
10
20
% Gravel (> 2000 µm)
% Mud (< 63 µm)

Fig. 11

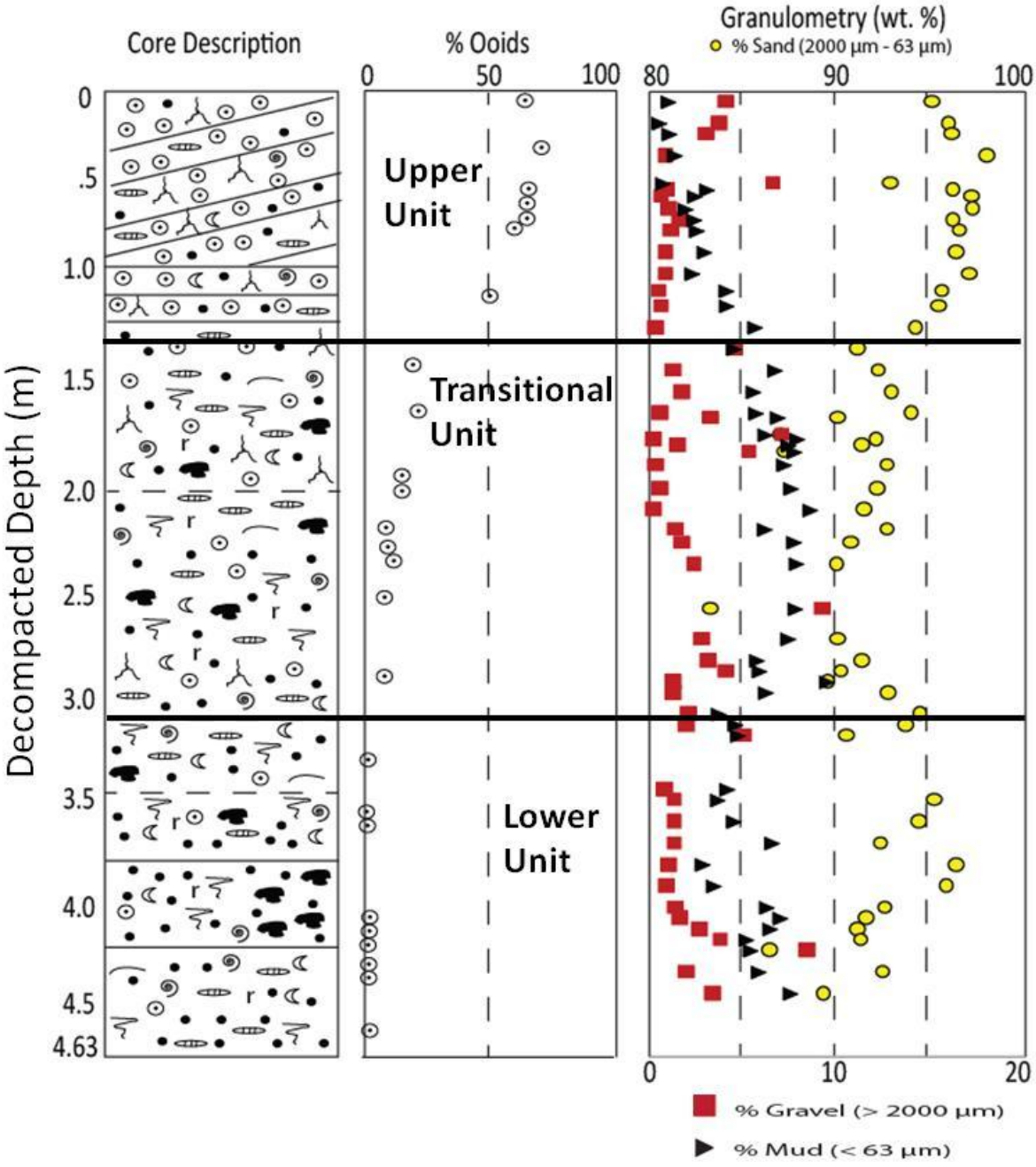
Core Description
% Ooids
0
50
100
Granulometry (wt. %)
% Sand (2000 µm - 63 µm)
80
90
100
Upper Unit
Transitional Unit
Lower Unit
Decompacted Depth (m)
0
.5
1.0
1.5
2.0
2.5
3.0
3.5
4.0
4.5
4.63
0
10
20
% Gravel (> 2000 µm)
% Mud (< 63 µm)

Fig. 12

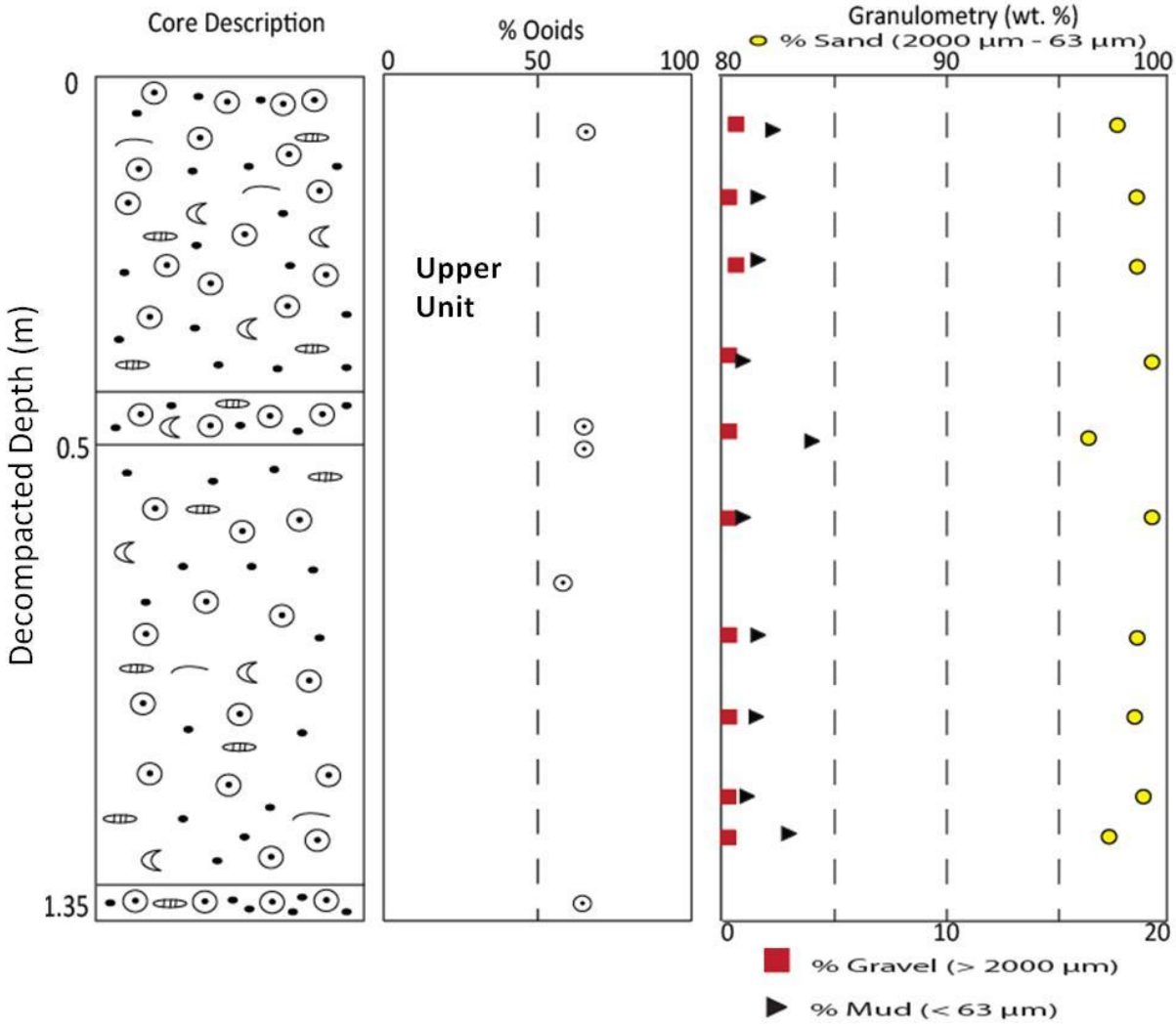
Core Description
% Ooids
0
50
100
Granulometry (wt. %)
% Sand (2000 µm - 63 µm)
80
90
100
Decompacted Depth (m)
0
0.5
1.35
Upper
Unit
0
10
20
% Gravel (> 2000 µm)
% Mud (< 63 µm)

Fig. 13

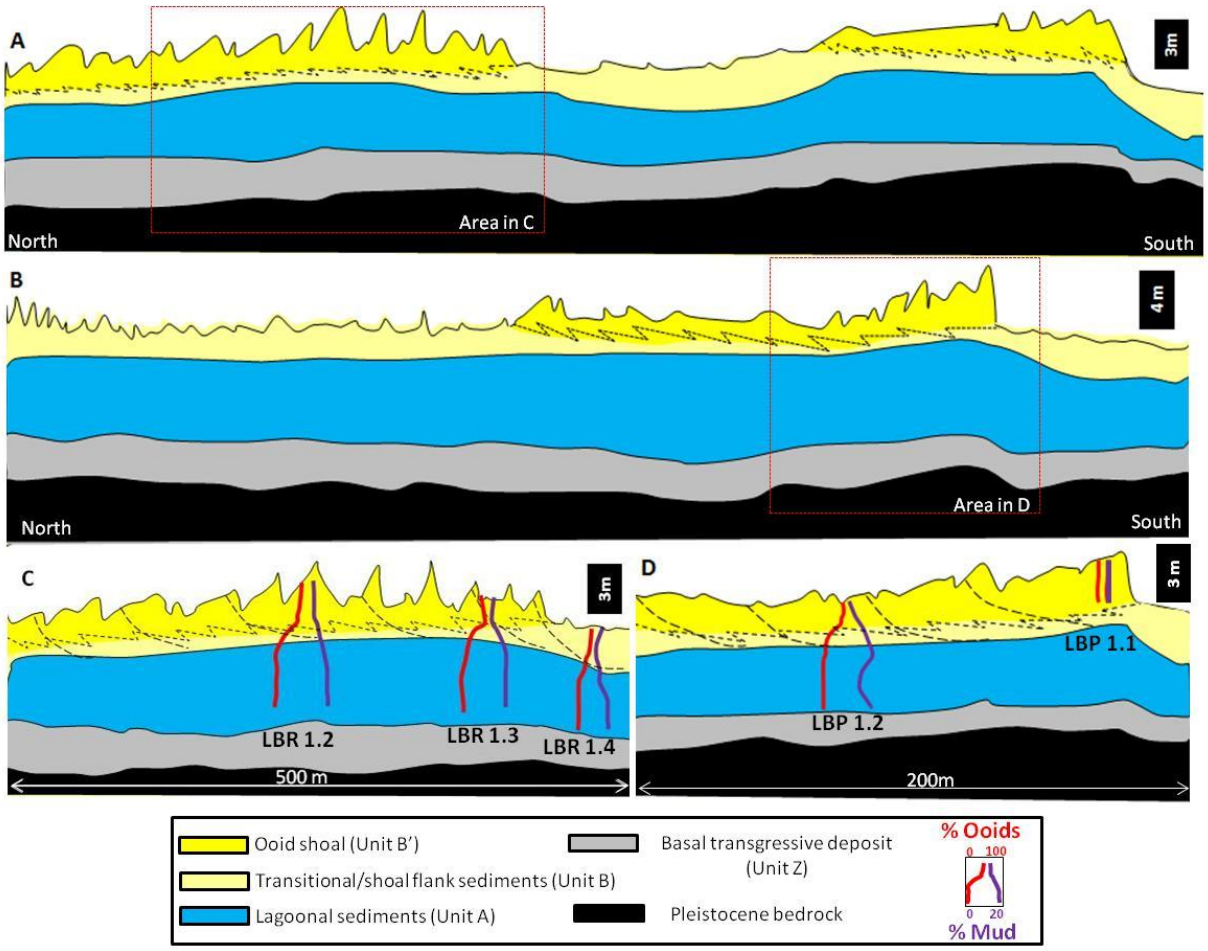
A
3m
Area in C
North
South
B
4 m
Area in D
North
South
C
3m
LBR 1.2
LBR 1.3
LBR 1.4
500 m
D
3 m
LBP 1.1
LBP 1.2
200m
Ooid shoal (Unit B')
Transitional/shoal flank sediments (Unit B)
Lagoonal sediments (Unit A)
Basal transgressive deposit (Unit Z)
Pleistocene bedrock
% Ooids
0 100
0 20
% Mud

Fig. 14

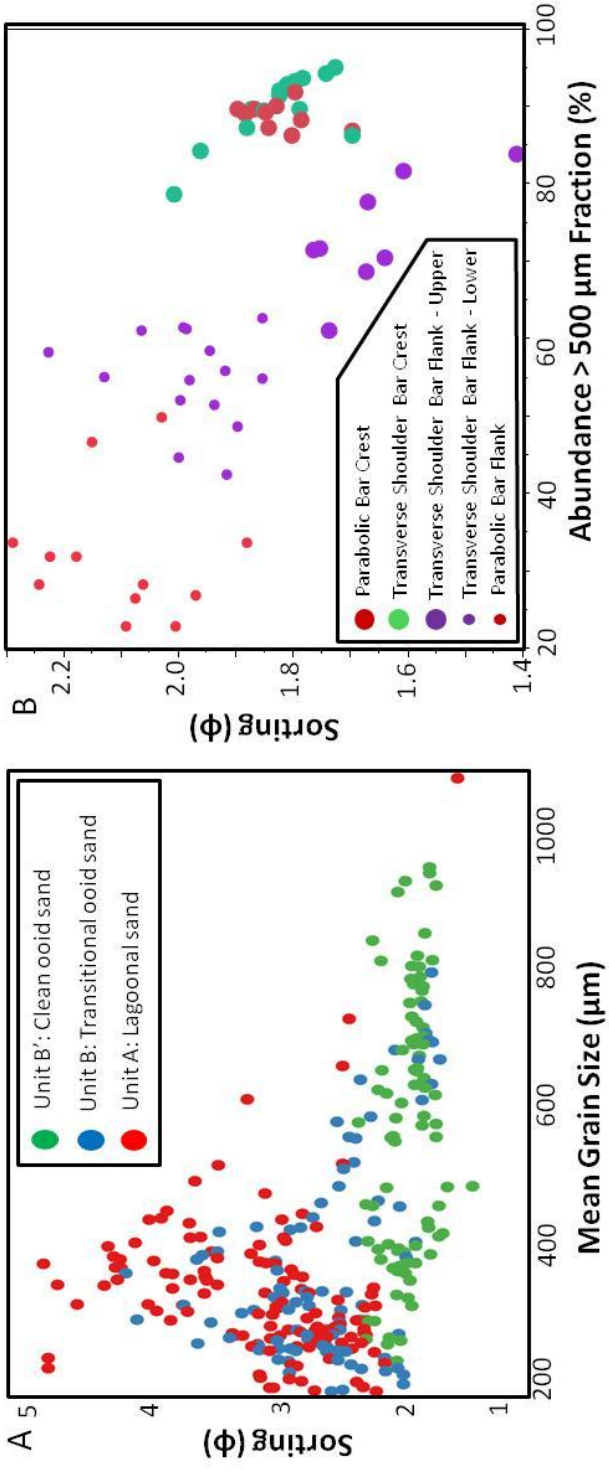
A
Sorting (ϕ)
Mean Grain Size (µm)
Unit B': Clean ooid sand
Unit B: Transitional ooid sand
Unit A: Lagoonal sand
B
Sorting (ϕ)
Abundance > 500 µm Fraction (%)
Parabolic Bar Crest
Transverse Shoulder Bar Crest
Transverse Shoulder Bar Flank - Upper
Transverse Shoulder Bar Flank - Lower
Parabolic Bar Flank

Fig. 15

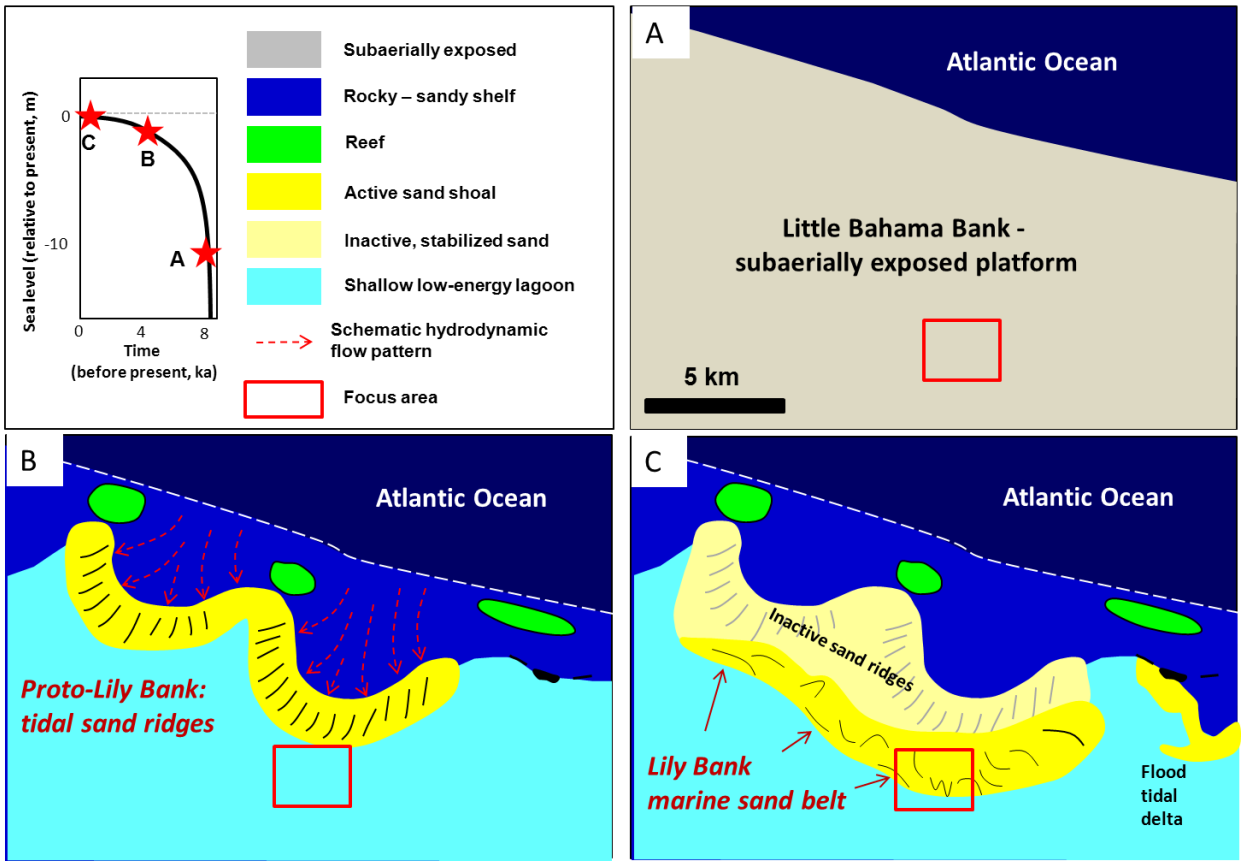
Sea level (relative to present, m)
0
-10
C
B
A
0
4
8
Time
(before present, ka)
Subaerially exposed
Rocky – sandy shelf
Reef
Active sand shoal
Inactive, stabilized sand
Shallow low-energy lagoon
Schematic hydrodynamic flow pattern
Focus area
A
Atlantic Ocean
Little Bahama Bank -
subaerially exposed platform
5 km
B
Atlantic Ocean
Proto-Lily Bank:
tidal sand ridges
C
Atlantic Ocean
Inactive sand ridges
Lily Bank
marine sand belt
Flood
tidal
delta

Fig. 16

APPENDICES

Appendix A: Core Descriptions

LBR 1.1

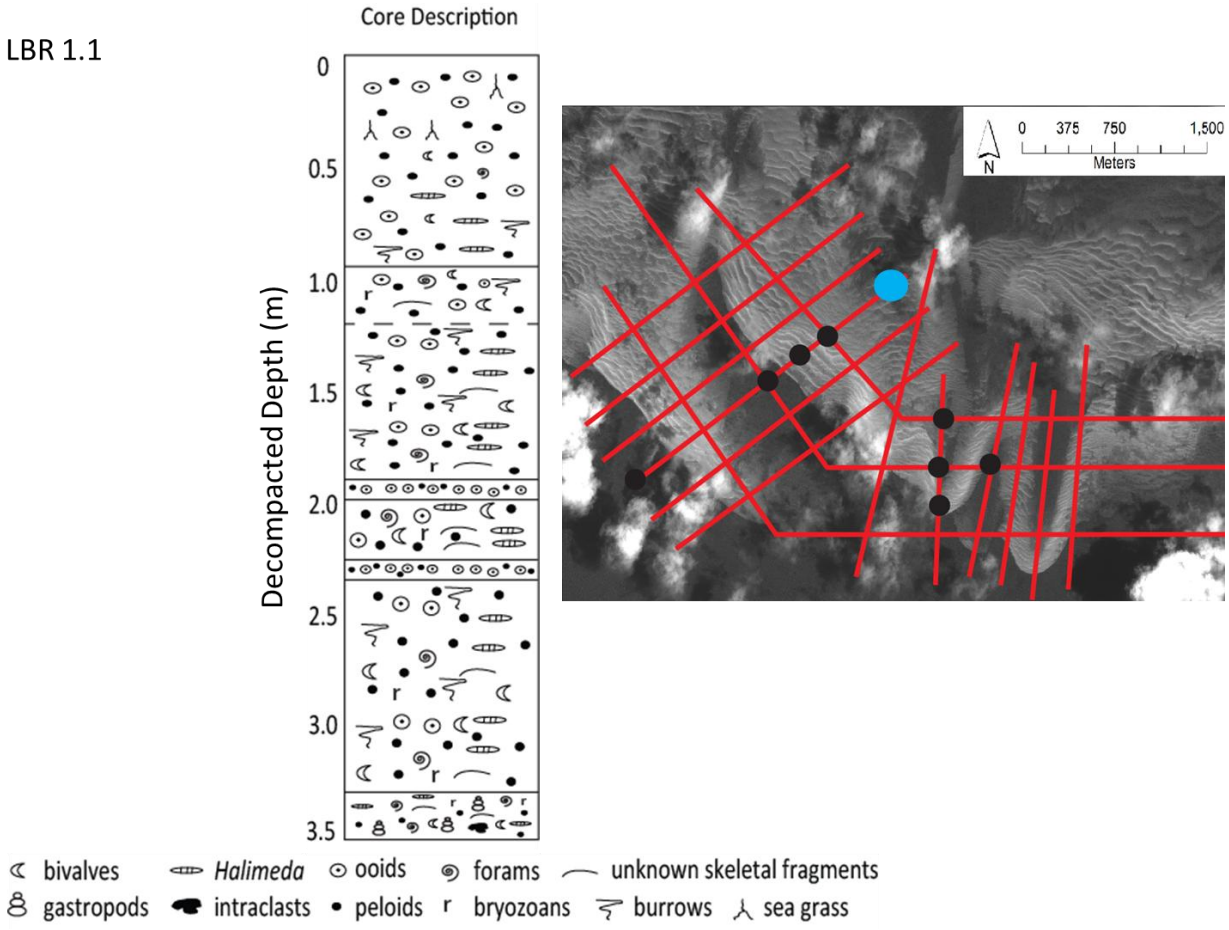

LBR 1.2

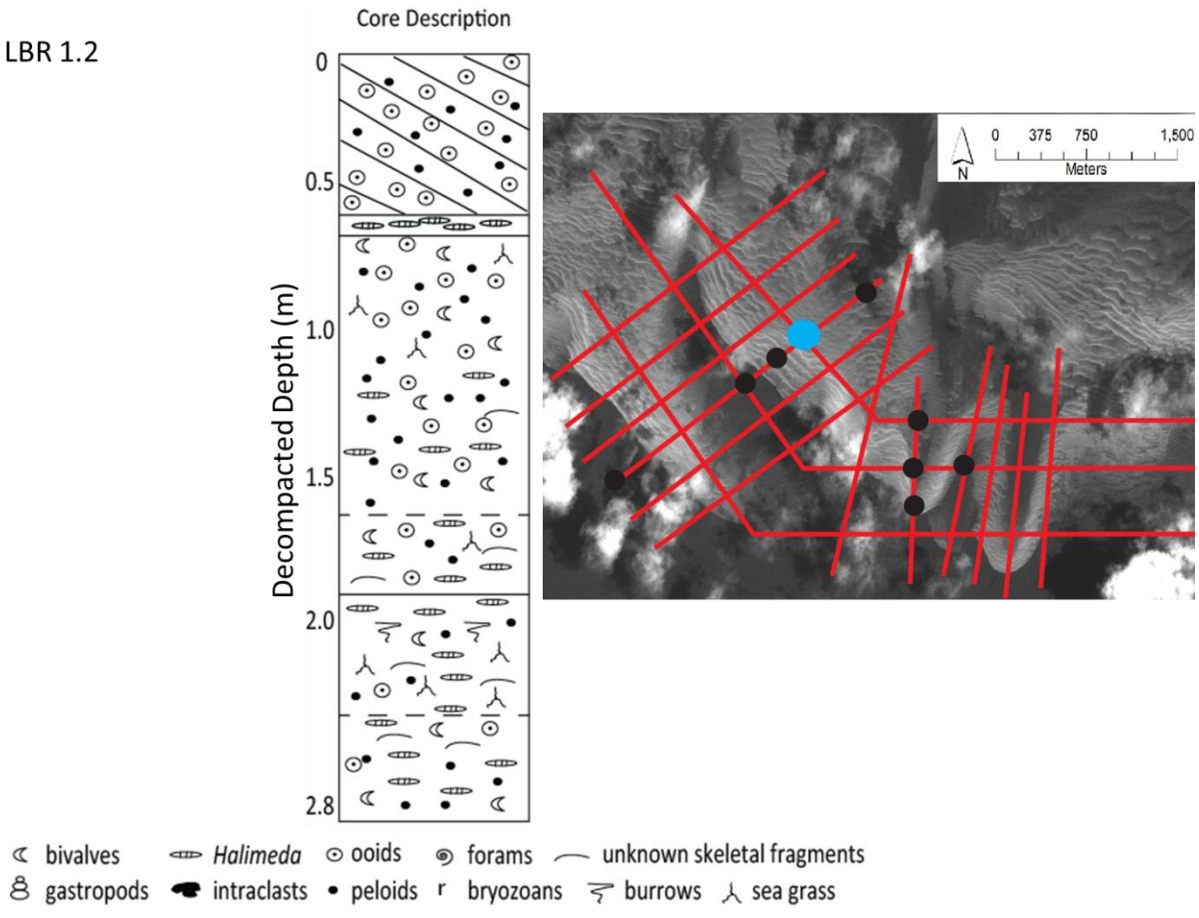
Core Description
Decompacted Depth (m)
0
0.5
1.0
1.5
2.0
2.8
0 375 750 1,500
Meters
N
bivalves
Halimeda
ooids
forams
unknown skeletal fragments
gastropods
intraclasts
peloids
bryozoans
burrows
sea grass

LBR 1.3

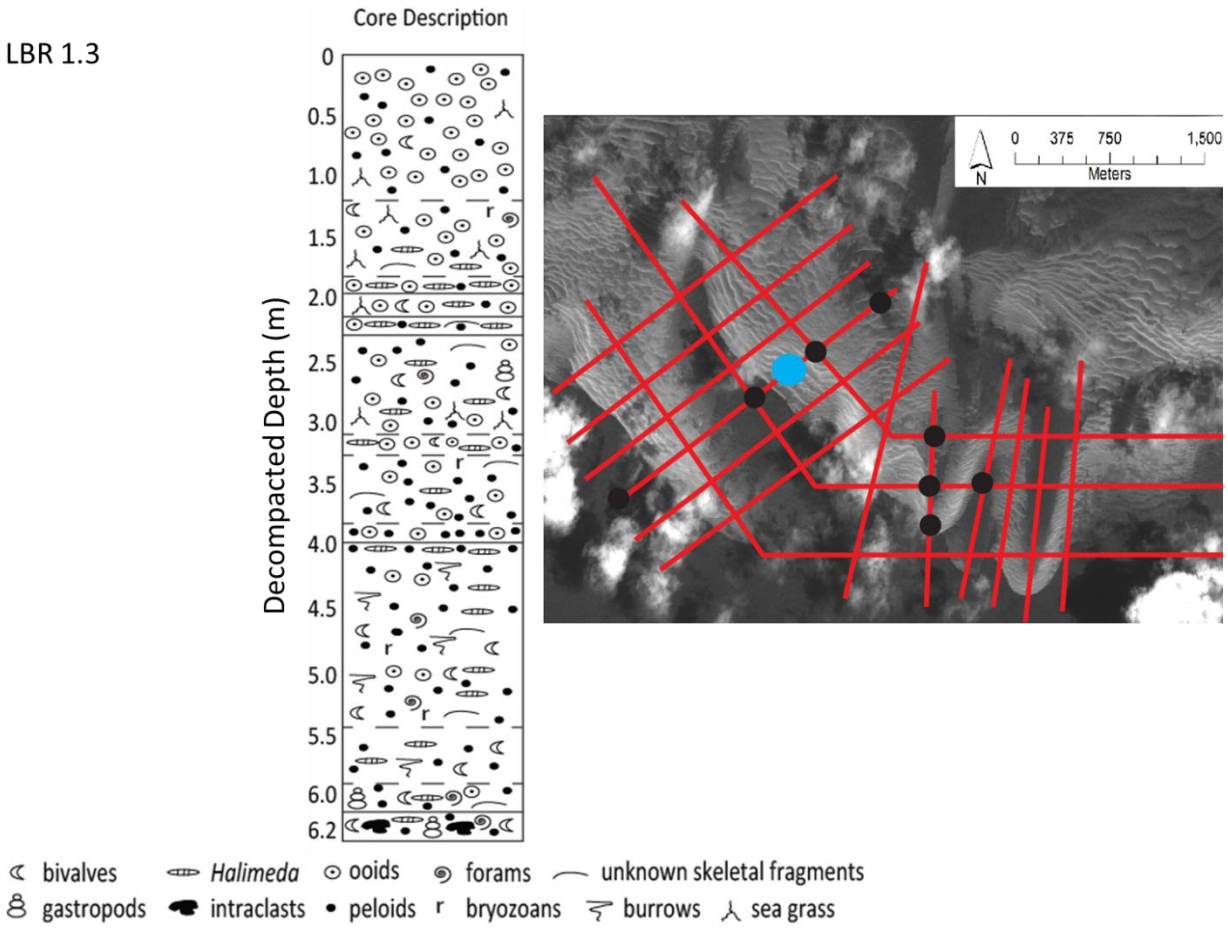
Core Description
Decompacted Depth (m)
0
0.5
1.0
1.5
2.0
2.5
3.0
3.5
4.0
4.5
5.0
5.5
6.0
6.2
r
0
375
750
1,500
Meters
N
bivalves
Halimeda
ooids
forams
unknown skeletal fragments
gastropods
intraclasts
peloids
bryozoans
burrows
sea grass

LBR 1.4

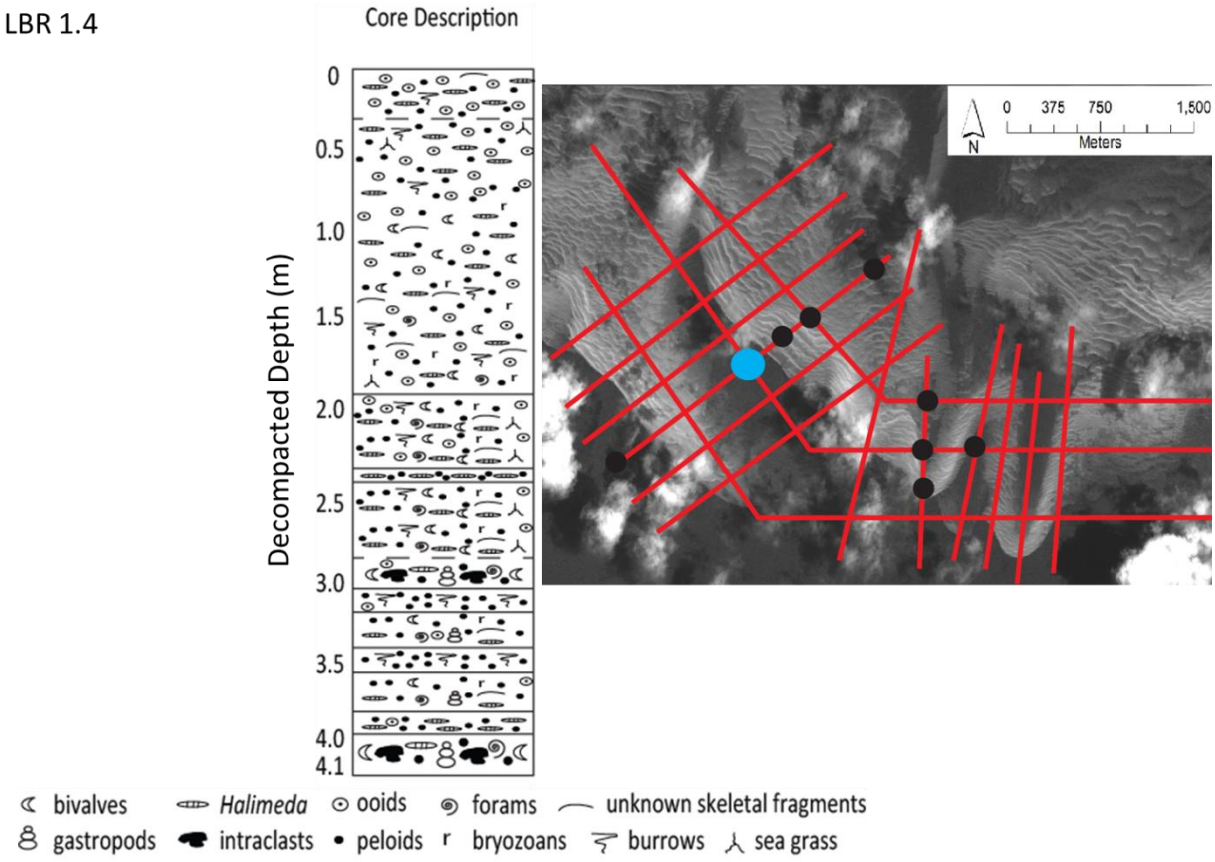
Core Description
Decompacted Depth (m)
0
0.5
1.0
1.5
2.0
2.5
3.0
3.5
4.0
4.1
0
375
750
1,500
Meters
N
bivalves
Halimeda
ooids
forams
unknown skeletal fragments
gastropods
intraclasts
peloids
r
bryozoans
burrows
sea grass

LBR 3.4

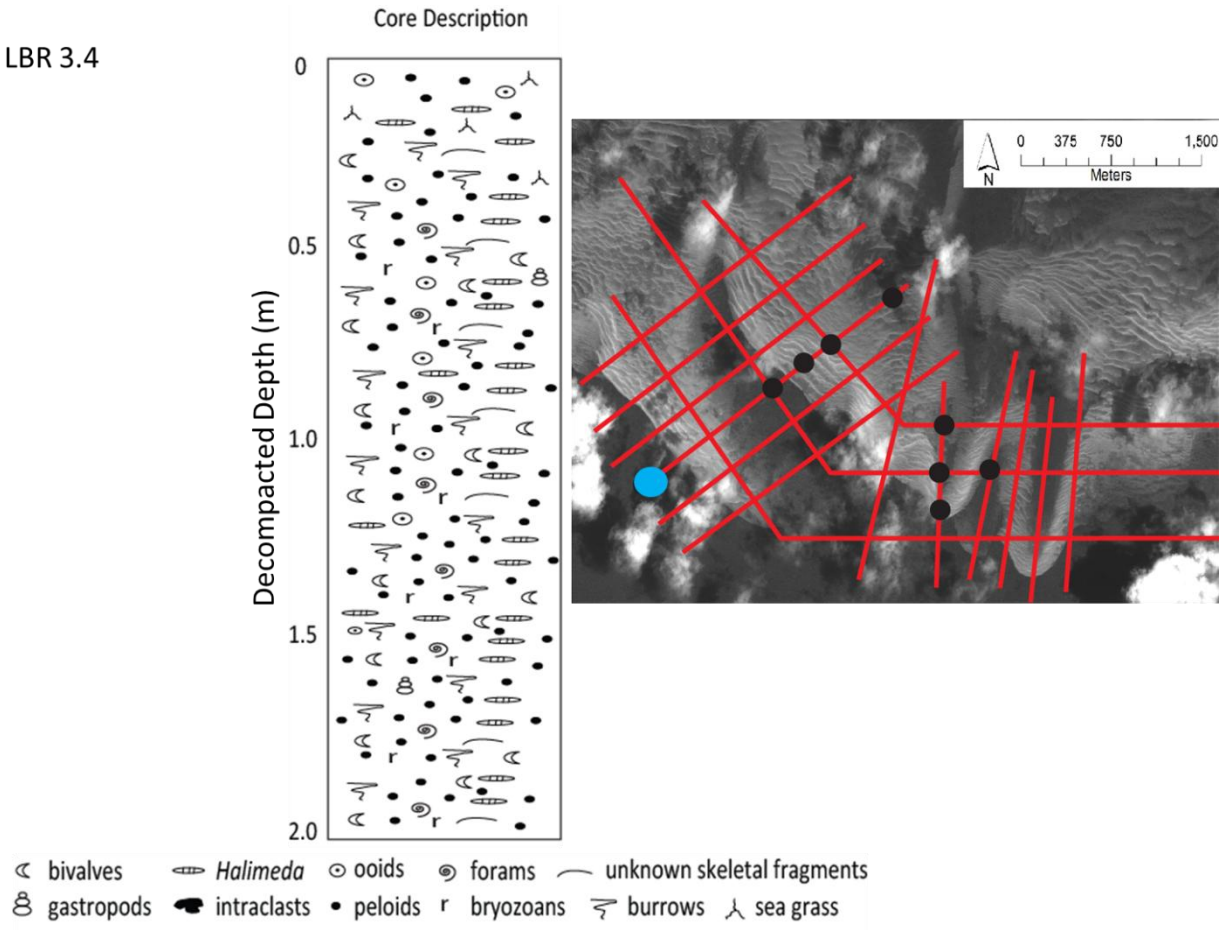
Core Description
Decompacted Depth (m)
0
0.5
1.0
1.5
2.0
0
375
750
1,500
Meters
N
bivalves
Halimeda
ooids
forams
unknown skeletal fragments
gastropods
intraclasts
peloids
bryozoans
burrows
sea grass

LBP 1.3

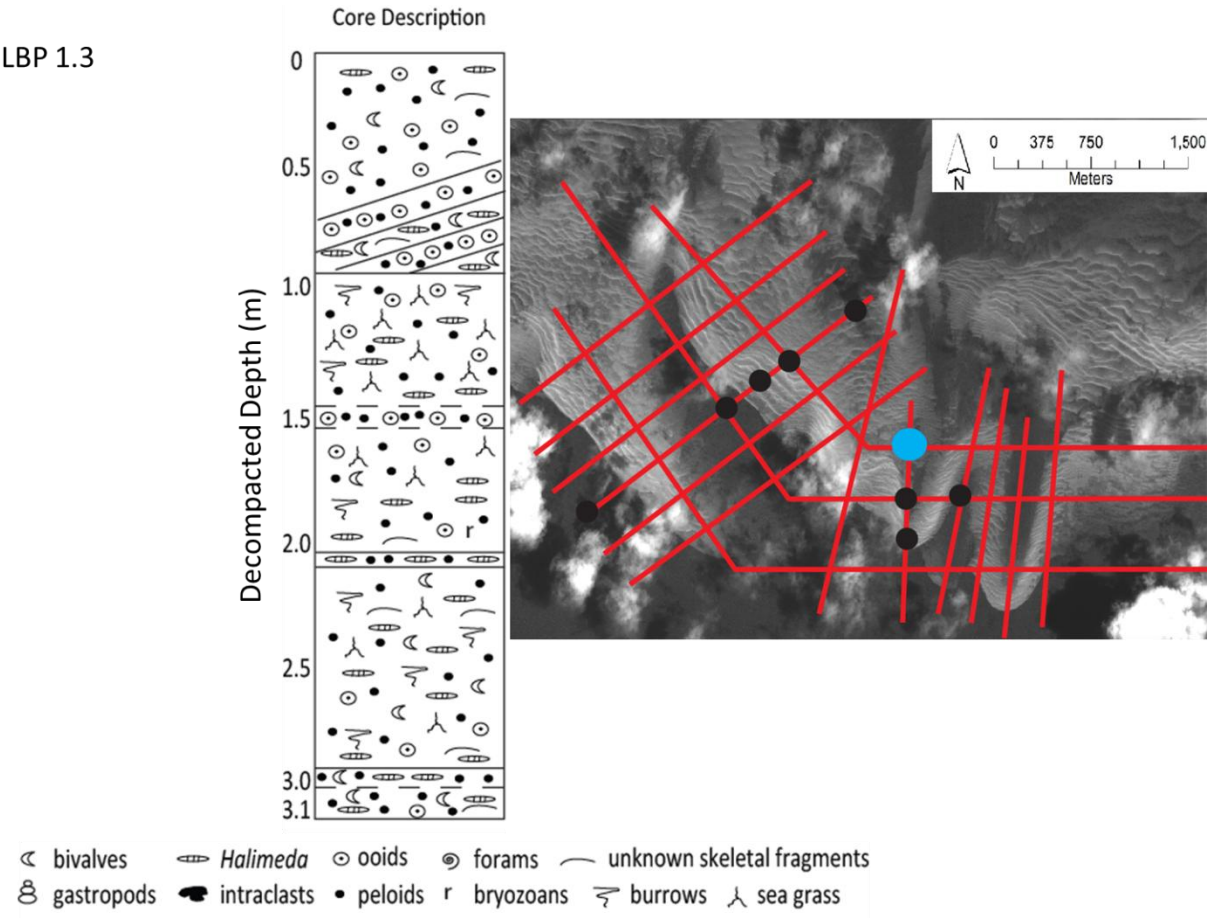
Core Description
Decompacted Depth (m)
0
0.5
1.0
1.5
2.0
2.5
3.0
3.1
r
0 375 750 1,500
Meters
N
bivalves
Halimeda
ooids
forams
unknown skeletal fragments
gastropods
intraclasts
peloids
r bryozoans
burrows
sea grass

LBP 1.2

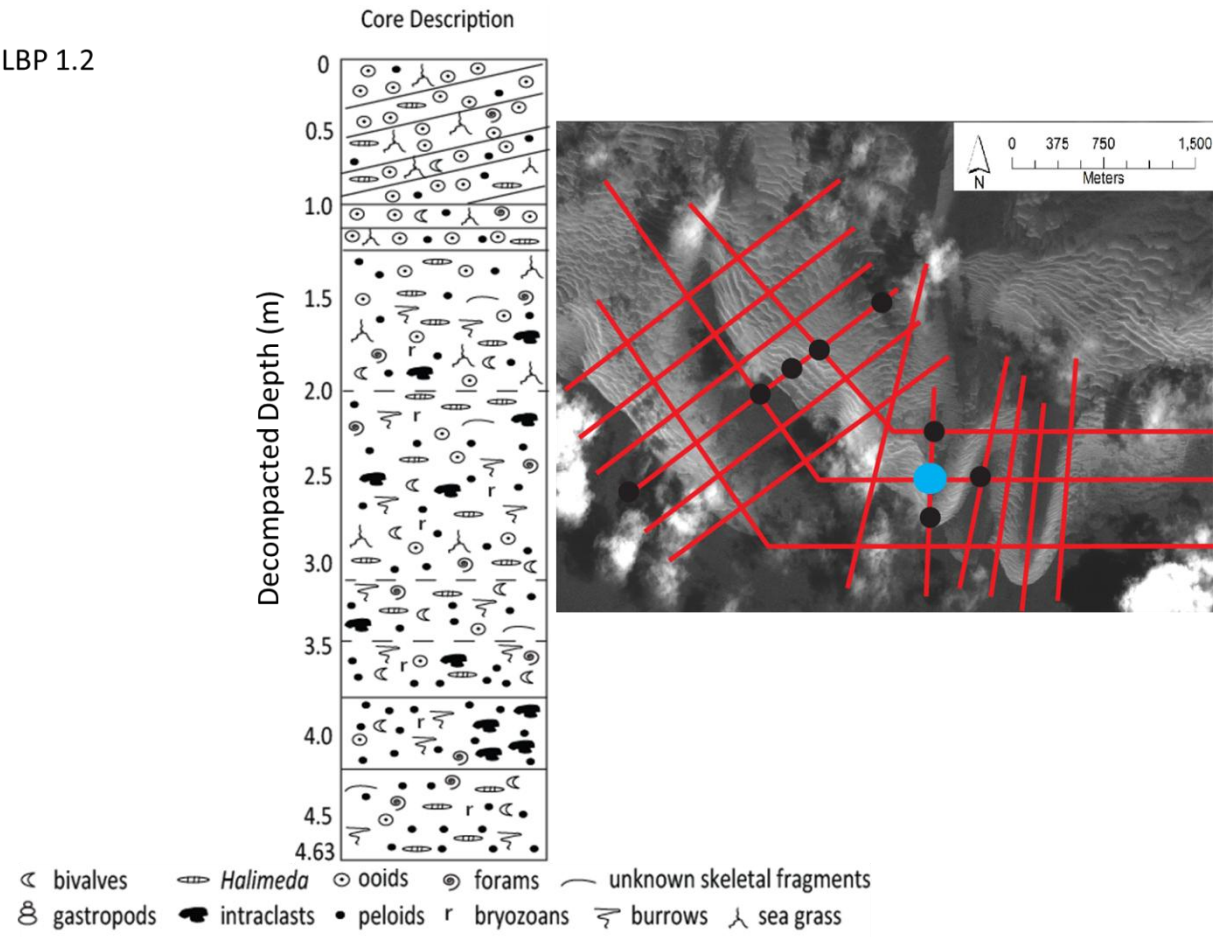
Core Description
Decompacted Depth (m)
0
0.5
1.0
1.5
2.0
2.5
3.0
3.5
4.0
4.5
4.63
N
0 375 750 1,500
Meters
bivalves
Halimeda
ooids
forams
unknown skeletal fragments
gastropods
intraclasts
peloids
r bryozoans
burrows
sea grass

LBP 1.1

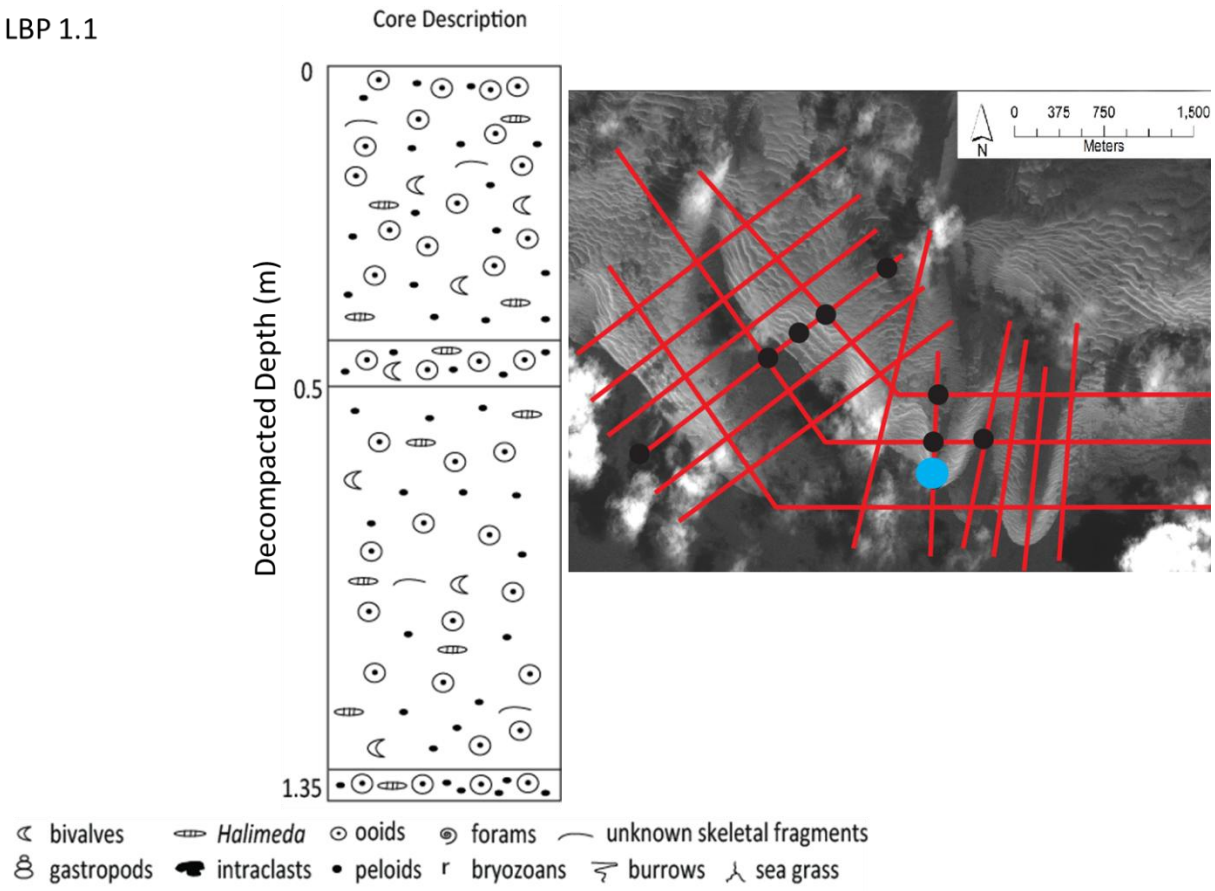
Core Description
Decompacted Depth (m)
0
0.5
1.35
0 375 750 1,500
Meters
N
bivalves
Halimeda
ooids
forams
unknown skeletal fragments
gastropods
intraclasts
peloids
bryozoans
burrows
sea grass

LBP 2.2

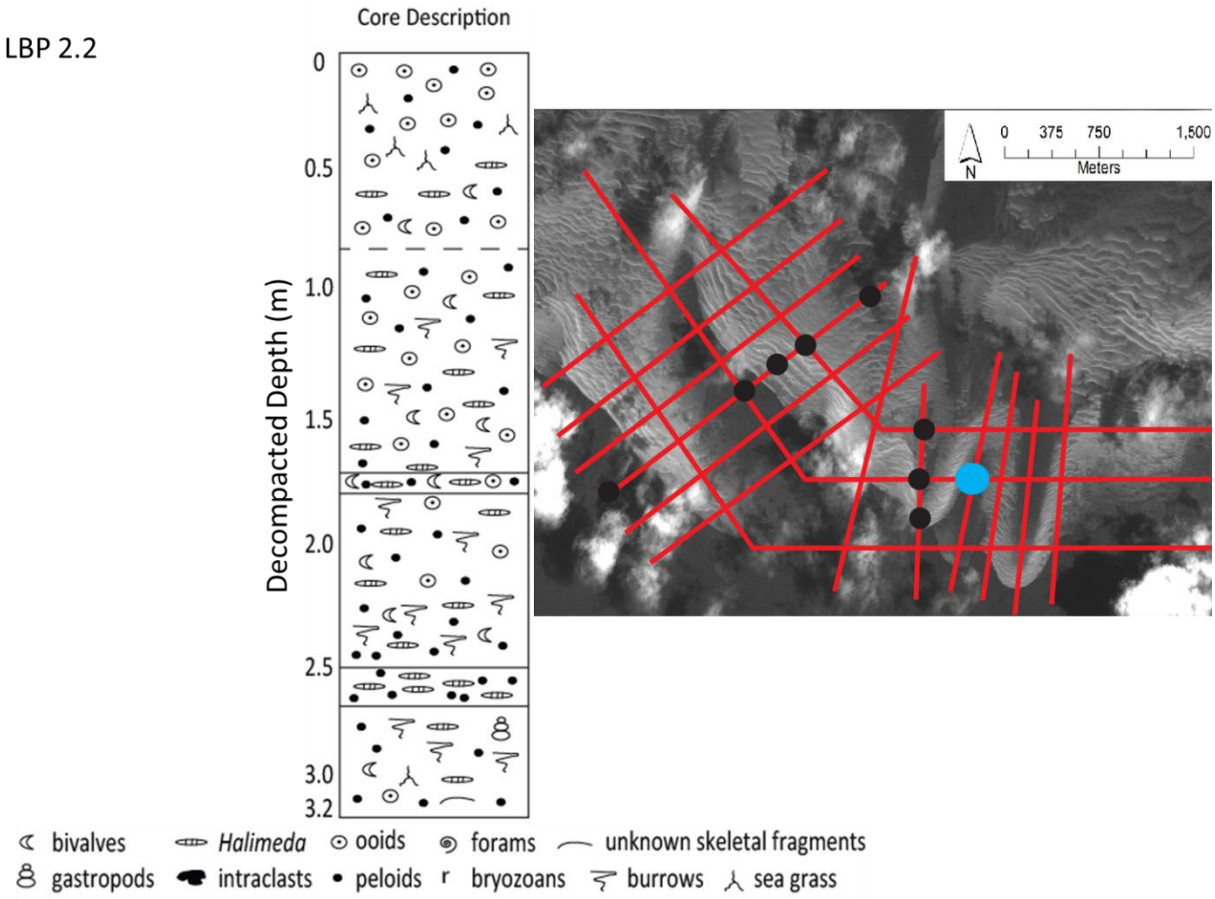
Core Description
Decompacted Depth (m)
0
0.5
1.0
1.5
2.0
2.5
3.0
3.2
N
0 375 750 1,500
Meters
bivalves
Halimeda
ooids
forams
unknown skeletal fragments
gastropods
intraclasts
peloids
bryozoans
burrows
sea grass

Appendix B: Core petrographic and granulometric data

This data is available upon request. Please contact:

Andrew G. Sparks
Email: asparks51@gmail.com

Or

Dr. Eugene C. Rankey
Email: grankey@ku.edu